# ChemComm

Accepted Manuscript


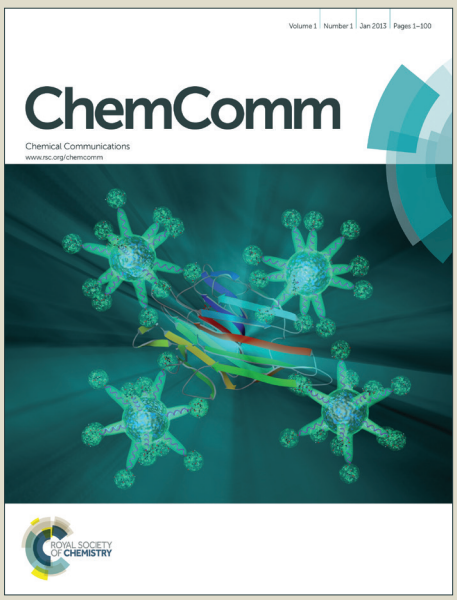





ROYAL SOCIETY OF CHEMISTRY

www.rsc.org/chemcomm

ChemComm

RSCPublishing

FEATURE ARTICLE

# Multiple Interfaces in Self-assembled Breath Figures

Cite this: DOI: 10.1039/xoxxoooooox

Ling-Shu Wan,* Liang-Wei Zhu, Yang Ou and Zhi-Kang Xu

Received ooth January 2012,
Accepted ooth January 2012

DOI: 10.1039/xoxxoooooox

www.rsc.org/

This feature article describes the multiple interfaces in the breath figure (BF) method toward functional honeycomb films with ordered pores. If a drop of polymer solution in a volatile solvent such as carbon disulphide is placed in a humid environment, evaporative cooling leads to self-assembled arrays of condensed water droplets. After evaporation of the solvent and water, patterned pores can be formed. During this BF process, the interfaces between the solution and substrate, the solution and water droplets, and the film surface and air play extremely important roles in determining both the structures and functions of the honeycomb films. Progress in the BF method is reviewed by emphasizing the roles of the interfacial interactions. The applications of hierarchical and functional honeycomb films in separation, biocatalysis, biosensing, templating, stimuli-responsive and adhesive surfaces are also discussed.

## 1. Introduction

Inspired by water droplet arrays formed on cold substrates,[1,2] the breath figure (BF) method has been utilized as a very simple and efficient technique for preparing films with ordered pores.[3] They are also called honeycomb films because the pores are often hexagonally close-packed. Widawski, Francois and coworkers first applied this method to the creation of honeycomb polymeric films by casting solutions of star polymers in carbon disulphide ($CS_2$) under a flow of moist gas.[3] The procedure and operation is very simple, but the exact mechanism behind this method is believed to be very complex. At present, it is generally accepted that this non-equilibrium method may involve the following processes: when a drop of polymer solution in a volatile solvent is cast on a substrate under humid conditions, evaporative cooling leads to condensation of water droplets onto the solution surface; the water droplets form stabilized polymer/water interface via adsorption or deposition of the polymer to prevent coalescence; then the water droplets grow bigger, possibly sink into the solution because of Marangoni convection and thermocapillary effects, and arrange into ordered two- or three-dimensional (2D or 3D) arrays; and finally a film with ordered porous structure is obtained after the solvent and water is thoroughly evaporated (**Fig. 1**).[4,5]

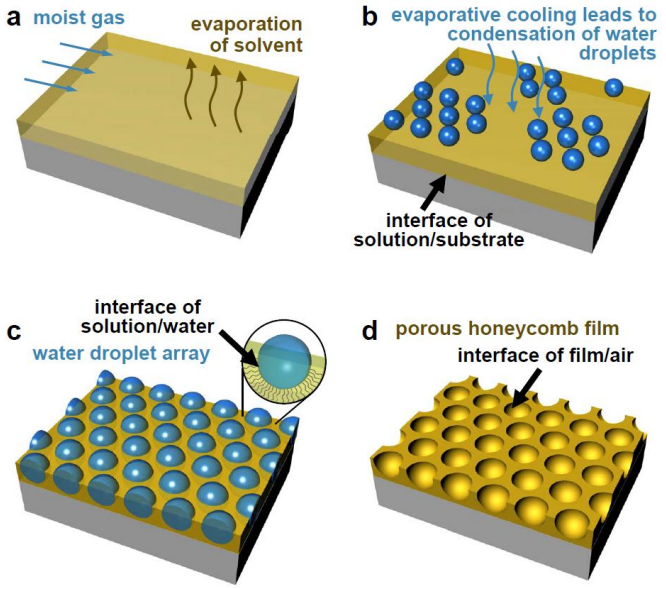


**Fig. 1** A possible model for the formation of honeycomb films by the breath figure method and the multiple interfaces.

*Ling-Shu Wan obtained his PhD degree in polymer chemistry and physics from Zhejiang University in 2007. Then he joined the Department of Polymer Science and Engineering of Zhejiang University and was promoted to an Associate Professor in 2009. He was a postdoctoral scholar in Prof. Paul F. Nealey's group at the University of Chicago. Dr. Wan's research interests include controlled polymerization, self-assembled polymeric films, and polymeric separation membranes.*

*Liang-Wei Zhu received his BS degree in applied chemistry from Xiangtan University in 2011. Then he joined the Department of Polymer Science and Engineering of Zhejiang University to pursue his PhD degree in Polymer Chemistry and Physics under the supervision of Dr. Ling-Shu Wan. His current research interests focus mainly on controlled synthesis of functional polymers for breath figure films.*

*Yang Ou received his BE degree in polymer science and engineering from Zhejiang University in 2011. Then he continued to pursue his PhD degree in polymer chemistry and physics at the same university under the supervision of Dr. Ling-Shu Wan and Prof. Zhi-Kang Xu. His current research interests are focused on advanced polymeric separation membranes with controllable pores.*

*Dr. Zhi-Kang Xu is a Qiushi distinguished professor at Zhejiang University. He received his PhD degree in polymer chemistry and physics at the Chemistry Department of Zhejiang University in 1991. He was financed by the National Natural Science Foundation of China for Young Distinguished Scholars in 2006. He is now on the editorial board of the Journal of Membrane Science. His research interests focus on the surface engineering of polymer membranes.*

In the past two decades, there has been tremendous progress in the BF method as briefly summarized below.[6-14] a) Various modified BF techniques have been reported for the preparation of honeycomb films.[11] The originally and most widely used method is the so-called dynamic or airflow technique, i.e., a moist airflow blows over the cast solution to facilitate solvent evaporation and bring water for condensation. Based on the same principle of use of water droplets as templates, some other techniques have been developed, for example, the static method in which the cast solution is confined in an airtight container with a humid environment,[15-29] the spin-coating technique,[30-36] the dip-coating technique,[37,38] and the emulsion technique.[37,39-42] b) Film-forming materials have been greatly expanded from star polymers[3,43-46] to linear block copolymers,[19,21,34,47-55] random copolymers,[35,56-60] linear polymers with polar end group,[61-64] homopolymers and PS without polar end groups,[18,65-67] dentrimers and hyperbranched polymers,[68-73] comb-like polymers,[74] biodegradable polymers,[75-79] conjugated polymers,[80-84] polymer blends,[85-90] hybrids of polymer and nanoparticles, microgels or even only inorganic materials,[91-116] and small molecules and supramolecular polymers.[23,117-123] The abundant materials enable a versatile BF approach to advanced functional honeycomb films. c) Different substrates have been used for film formation, which include a wide variety of flat or rough solid substrates,[124-126] surfaces with 3D structures,[20,24,28,44,127-133] and even liquids.[94,98,134-137] The properties of substrates can affect the film structure. d) New structures continue to emerge. For instance, in addition to films having spherical pores and monolayer structure, those with U-shaped pores[29,138,139] and multilayer structure[140,141] are controllable. It is also interesting to produce films with through pores, 3D conformal micropatterns, and hierarchical structures in the pores. e) More and more potential applications have been exploiting. Up to now, it has been demonstrated that honeycomb films are valuable in the fields of templating and microfabrication,[15,142-145] biomaterials,[146-149] superhydrophobic surfaces,[26,150,151] sensing,[152] catalysis,[153] separation,[137,154] responsive surfaces,[16] coatings,[155] surface enhanced Raman scattering (SERS) substrates,[85,156] microchannels,[157] optical and conductive materials.[122,158-160]

We would like to point out that during the BF process the multiple interfaces between the solution and substrate, the solution and water droplets, and the film surface and air (**Fig. 1**) play extremely important roles in determining the structures and functions of honeycomb films. The importance of solution/water droplets interface has been well recognized as it governs the formation of honeycomb films regardless of building blocks used. The interfacial behaviors of building blocks, such as polymers with polar group or blocks, blends, nanoparticles, and reactive components, endow honeycomb films with hierarchical structures and advanced functions. The role of solvents, the interfacial tension, the use of non-aqueous vapor as well as the characterization of interfacial chemistry is also discussed at this interface. The solution/substrate interface has received much less attention although it is also crucial to the structures and functions of honeycomb films. At this interface we emphasize BFs on liquid surfaces and non-planar substrates following a brief summary of the effects of solid substrates. The highly porous surfaces of honeycomb films may possess very interesting interfacial phenomena. Here we highlight some examples of superhydrophobic surfaces, surfaces with wetting transition, adhesive surfaces, and stimuli-responsive surfaces. The related applications of the films are also included in each section.

In this feature article, we focus on the above-mentioned interfaces that may induce beautiful structures, advanced functions, and exciting applications. For the history and development of the BF method,[6-8] some related special topics such as the combination with phase separation[13] and unconventional fabrication,[14] or more detailed information and progress,[11,12] please refer to the corresponding reviews.

## 2. Interfaces between substrates and solutions

### 2.1 Solid substrates

The first report of honeycomb films is on a flat solid surface.[3] Up to now, various solid substrates have been used, including glass, silicon wafer, mica, and polymeric films such as poly(ethylene terephthalate) (PET), polyethylene (PE), and polyvinylchloride (PVC).[124] Solid substrates generally result in films with a bilayer structure, i.e., a top porous layer and a bottom dense layer,[3] although films with through pores have been reported on a glass substrate where a modified BF method was adopted by introducing a sucking process.[161] Therefore, it may be speculated that the condensed water droplets at the solution/air interface do not directly contact with the solid substrate. However, results indicate that the surface properties of solid substrates can affect the film formation indeed. An early example reported by Xi et al. is the formation of honeycomb films on hydrophilic substrates including mica, glass, and silicon.[125] They cast an amphiphilic dendronized block copolymer solution in chloroform onto these substrates. It was found that mica, on which water and polymer solution spread best, leads to the most regular film and the easiest film formation; in contrast, under the same condition they were not able to obtain ordered film on silicon surface. Results by Hu et al. on substrates with different hydrophilicity also support this conclusion.[50] Ferrari et al. further investigated the role played by both solvent and substrates in the BF process using a linear PS.[124] They compared a series of substrates with different surface free energies including fluorinated surface with a surface free energy as low as 13.8 mJ/m$^2$. It is hard to form ordered films on the scarcely wettable fluorinated surface. They contended that the role played by the substrates is strictly related to the type of solvent used. This relationship is surely possible, and probably it is also relevant to other factors even experimental operations such as the thickness of cast solution.[151] Moreover, it's worth pointing out that surface roughness may affect film formation as proved by the study



 

of water condensation on surfaces with similar surface free energies but different surface roughness.[126]

Interestingly, sometimes BFs can form square array instead of hexagonally close-packed array that is believed to have the lowest free energy. Such square patterns have been reported by Han,[65] Karthaus[162] and their coworkers occasionally or through flowing the solution over an inclined substrate during solvent evaporation and water condensation. Cai and Newby obtained porous polymer films with hexagonal and square arrangements by using a Marangoni flow-based method, which is slightly different from the traditional BF method but also uses condensed water droplets as templates.[163] They demonstrated the formation of hexagonal and square arrays on hydrophilic silicone oxide (SiO*x*) and relatively hydrophobic silicon (Si) substrates, which have a static water contact angle of 37.1 °and 76.3 °, respectively. However, as mentioned-above, square patterns are only very unusually observed in the traditional BF method. Considering the potential applications of square patterns in the semiconductor industry's integrated circuit design, software, and fabrication process, developing square arrays of BFs should be an interesting topic.

### 2.2 Liquid substrates

The substrates were first extended to liquid surfaces by, as far as we know, Parisi and coworkers.[134] Generally, in order to successfully form honeycomb films polymer solutions should spread well on the liquid surface, which is a premise. The conditions for spreading a drop of polymer solution over a liquid surface is determined by the surface thermodynamics, which can be described using a spreading coefficient *S*:[134]

$$S = \gamma_{sg} - (\gamma_{pg} + \gamma_{ps}) \quad (1)$$

where $\gamma_{sg}$ is the surface tension of liquid substrate; $\gamma_{pg}$ is the surface tension of polymer solution; and $\gamma_{ps}$ is the interfacial tension between the polymer solution and the liquid substrate. $S \geq 0$ means complete wetting whereas $S < 0$ indicates partial wetting. By a simple qualitative analysis we know that liquids with large surface tension (e.g., water) will be beneficial to the spreading of polymer solution. Parisi et al. prepared honeycomb films with through pores from conjugated polymers using a 40% water solution of saccharose as the substrate fluid, which has even higher surface tension (84.0 mN/m) than pure water (72.8 mN/m at 20 ℃).[134] A typical work by Shimomura and coworkers reported large area honeycomb films from an amphiphilic copolymer on the surface of Milli-Q grade water.[135] They confirmed the through-pore structure by scratching in atomic force microscopy (AFM) measurement. As the surface tension of water increases with lowering the temperature, the film area increases with the decrease in water temperature. They applied the free-standing honeycomb film to cell culture. Another kind of intriguing film-forming materials is inorganic particles. As early as 2005, Wu et al. started to investigate the self-assembly of polyoxometalates (POMs) into well-patterned honeycomb architectures on solid surfaces.[164] Hao and coworkers fabricated highly ordered honeycomb films of a POM at the interface of air/water.[94] The concentration of surfactant was found to be critical to the ordered structure of the films; only moderate concentration of surfactant leads to a perfect honeycomb structure. Hao group further investigated the self-assembly of a series of POMs and other nanoparticles such as gold nanoparticles and nanocomposites at the interface of air/water.[92,99,165,166] More recently, Chen et al. fabricated free-standing graphene honeycomb films on water surface and revealed that the films exhibit superior broad-spectrum antibacterial activity.[98] It should be noted that all of the above-mentioned work used a so-called "double-casting" method in which a small amount of polymer solution or surfactant is cast on the water surface in advance to ensure that a polymer solution for film preparation can form a stable liquid film on water surface.

Water is the most commonly used liquid substrate in the BF process. According to equation (1), organic liquids on which polymer solutions spread well may theoretically be the candidates. Wang et al. discovered early that PS in tetrahydrofuran (THF) can form patterned porous films on the surface of ethylene glycol that has a surface tension of ~46.5 mN/m,[167] which is lower than that of water but is relatively high in organic solvents. According to their results, the films have multilayered pores open on only one side. They also pointed out that in their conditions (low relative humidity of 30-40% and even in a dry $N_2$ atmosphere) patterned porous films form only on the surface of ethylene glycol, not on a glass substrate. Considering both the effects of substrates and that the BF arrays can be formed at a rather low relative humidity of 30%,[68] the mechanism behind their process may involve but be more complex than the BF method.

We fabricated highly ordered honeycomb films with through pores by a "single-casting" technique on the surfaces of ice and other organic solvents including glycerol and formic acid.[137] Ice is a solid substrate; however, it tends to form a very thin layer of liquid water on its surface when it is put at room temperature. This characteristic makes polymer solution, at least our block copolymer polystyrene-*block*-poly(N,N-dimethylaminoethyl methacrylate) PS-*b*-PDMAEMA solution in $CS_2$, spread much better on ice than on bulk water surface. Thus, single-casting is feasible, i.e., polymer solution can be directly cast onto an ice surface without any underlying pre-cast thin films. The resultant ordered films can be easily transferred to other porous supporting materials, forming a composite membrane (**Fig. 2**). We demonstrated for the first time the concept of using such ordered composite membrane for size-selective separation of microspheres. Cong et al. also obtained honeycomb membranes from brominated poly(phenylene oxide) (PPO) on an ice surface and described the good permeation ability.[168] Because of the unique ordered structure, honeycomb films with through pores will be useful in a wide variety of fields such as separation, templating, and tissue engineering.

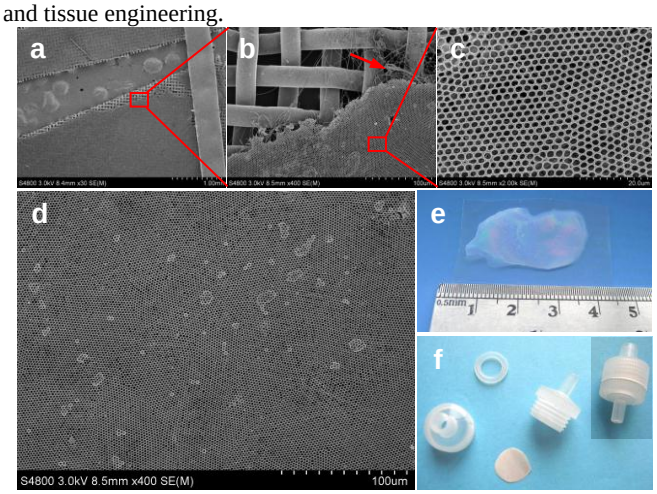


**Fig. 2** (a)–(d) SEM images of the composite membrane with different magnifications. (e) Digital photograph of a piece of ordered membrane. (f) Digital photographs of the composite membrane and the membrane module used for separation. From ref. 137. Copyright 2012 American Chemical Society.

It is an interesting question how through pores are easily produced on liquid surfaces. Parisi et al. proposed that there is a thin interface polymer film between drying polymer solution and the substrate, and the water droplets break through this thin film during the drying process.[134] They mentioned that such kind of penetrated polymer layers can usually be seen inside some pores. Shimomura et al.

claimed that it is related to the thickness of cast solution and the density of solvent.[135] We agree that the thickness of cast solution, which is determined by the amount of solution added and its ability to spread, is very important for the formation of through pores; thinner is better. Concerning the density of solvent used, it is more complicated. Not only benzene ($\rho$ = 0.87 g/mL) which has a smaller density than water (1.00 g/mL), but chloroform (1.48 g/mL) and $CS_2$ (1.26 g/mL) have been successfully utilized to prepare through-pore honeycomb films. It can be attributed to the thermocapillary effect and Marangoni convection which pull down the water droplets toward the bottom of polymer solution.[5] Moreover, the reported results imply some kind of link between the density of solvents and the final position of water droplets in the polymer solution. In other words, the shape of pores can be affected by the density of solvent (**Fig. 3**).[137]

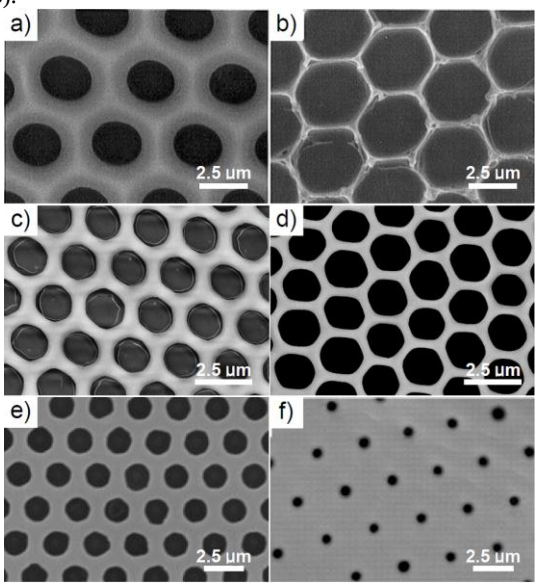


**Fig. 3** SEM images of the top (surface contacts with air, left panel) and bottom (surface contacts with water, right panel) surfaces of through-pore honeycomb films prepared using solvents with different density. (a,b) Benzene from ref. 135. (c,d) $CS_2$ from ref. 137. (e,f) chloroform from ref. 92.

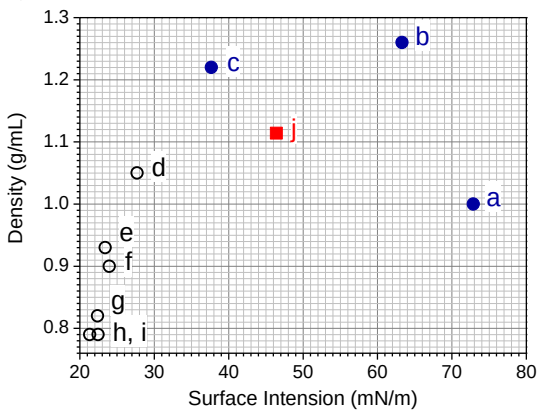


**Fig. 4** Effects of surface intensions and densities of liquids as substrates for honeycomb film formation. (a-c) Only filled circles refer to successful formation of honeycomb films with through pores: (a) water, (b) glycerol, and (c) formic acid. (d-i) Hollow circle: (d) acetic acid, (e) tetraethyl orthosilicate, (f) ethyl acetate, (g) ethanol, (h) isopropanol, and (i) methanol. From ref. 137. (j): ethylene glycol from ref. 167. See section 2.2 for details.

We prepared honeycomb films on the surfaces of a series of organic solvents, and results indicate that surface tension of the liquids is crucial to the formation of through pores. Organic solvents with relatively high surface tension such as glycerol and formic acid have contributed to the formation of honeycomb films with through pores (**Fig. 4**). It's worth noting that ethylene glycol used by Wang et al. also has a relatively high surface tension but in their work polymer solution with a very high concentration of 10 wt% was used.[167] During the BF process condensed water droplets self-assemble into hexagonal arrays and penetrate the polymer thin film between solution and substrate, if it is thin enough, to form through pores, which is reasoned by the excess of the surface tension differential pressure to the critical rupture pressure across the thin film.

### 2.3 Non-planar 2D or 3D substrates

In addition to surface physicochemical properties such as wettability, the morphology of substrates also plays an important role in fabricating advanced honeycomb films. Formation of honeycomb films on non-planar substrates produces well-designed hierarchically ordered films, which can be used as templates for soft lithography. Qiao et al. performed pioneering and systematic works by directly preparing hierarchically ordered films without using photolithography (**Fig. 5a**).[24,28,44,127-129] They synthesized a series of core-crosslinked star (CCS) polymers with different glass transition temperatures ($T_g$) and fabricated honeycomb films by placing a transmission electron microscopy (TEM) grid on glass surface before dropping polymer solution. The initial CCS polymers they used have rather low $T_g$, for example, -122 ℃[127] and 3 ℃.[128] Recently, they synthesized CCS polymers with $T_g$ ranging from 2 ℃ to 100 °C and with different Young's modulus to prepare non-cracking (or conformal) honeycomb films by a static casting method.[28] They obtained non-cracking honeycomb films on non-planar surfaces from polymers with $T_g$ values as high as 94.5 ℃. As a consequence, they concluded that the Young's modulus of a polymer is a more important factor, compared to $T_g$, in determining the occurrence of cracking during honeycomb film formation on non-planar surfaces. This finding is an interesting advance as it may provide access to the formation of honeycomb films from a variety of different polymers not used before. Kim et al. used a monocarboxy terminated PS to form honeycomb films.[130] This polymer may have a $T_g$ close to 100 ℃. They cast polymer solution

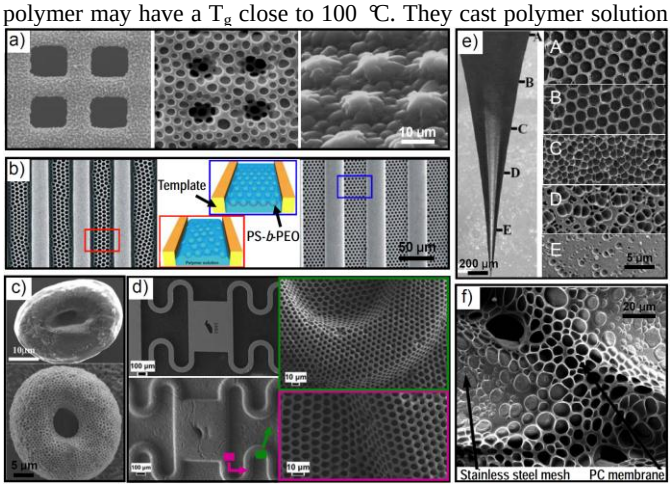


**Fig. 5** Some typical non-planar substrates for honeycomb film formation. (a) TEM grids from ref. 127. (b) copper grating from ref. 130. (c) 3D particles from ref. 128. (d) bas-relief silicon wafer from ref. 20. (e) 3D micropipette with curvature gradient from ref. 131. (f) 3D porous mesh from ref. 132.



 

on organically modified silicon wafer surface and then put a copper grating over the polymer solution to facilitate templated organization of the water droplets. They found that the addition of a polymeric surfactant that can improve interfacial wetting is crucial to the hierarchical structures (**Fig. 5b**).

3D substrates can also be "coated" with BFs other than "2D" non-planar substrates. Qiao et al. first reported formation of honeycomb films on some microspheres and irregular particles using a CCS polymer with a very low $T_g$ (-124 ℃) and obtained perfectly conformal BF films (**Fig. 5c**).[128] In another interesting experiment, Li et al. developed a robust strategy toward 3D honeycomb films from commercially available block copolymers such as polystyrene-*block*-polyisoprene-*block*-polystyrene (SIS) on various non-planar substrates (**Fig. 5d**).[20] After vulcanization, free-standing films can be obtained, and the films become resistant to a wide range of organic solvents and thermally stable up to 350 ℃. This strategy is valuable to highly stable films with 3D ordered structures. Gu et al. chose micropipette with curvature gradient as a substrate using poly(L-lactic acid) (PLA) as the film-forming polymer and dioleoylphosphatidylethanolamine (DOPE) as the surfactant.[131] They showed that the honeycomb structures including pore size and regularity change remarkably with the gradually increased surface curvature; at high curvatures several of the pores are extremely close to each other, forming "semi-coalescence" hemispherical pores strings (**Fig. 5e**). Using a dip-coating technique, honeycomb films with through pores were formed from polycarbonate (PC) on stainless steel gauzes (**Fig. 5f**), which exhibit Cassie-Wenzel wetting transition[132] and the potential in water/oil separation.[133] Films with through pores were also prepared on glass beads floated on water surface, but they are disordered to some extent.[169]

## 3. Interfaces between solutions and condensed water droplets

### 3.1 The role of solvents and the interfacial tension

It has been accepted that star polymers (and other polymers) are able to precipitate at the interface of polymer solution and water droplets to stabilize the water droplets.[8] One of the keys to ordered honeycomb films is to prevent water droplets from coalescing. Therefore, the interfacial tension between polymer solution and water droplets plays a crucial role in determining the structures of honeycomb films, for example, regularity, pore shape, and mono- or multilayer structures.

Ferrari et al. proposed that the thermodynamic affinity (Hansen solubility parameters, HSP) between polymer and solvent is the key parameter for BFs formation, along with other solvent characteristics such as water miscibility, boiling point, and enthalpy.[124] On the other hand, Fukuhira et al. studied the effects of interfacial tension on the formation of self-assembled honeycomb films by adding surfactants with different hydrophile-lipophile balance (HLB) values.[170] They found that the stability of water droplets in the solution is affected to a large degree by the surfactants. The HLB value and interfacial tension are important parameters affecting droplet stability. They concluded that surfactant that has a HLB value of lower than 6.5 and can maintain high interfacial tension (>10 mN/m) will facilitate formation of ordered honeycomb films. It is reasonable because the BF process can be considered as a water-in-oil system where surfactants with a low HLB value are preferred. It should be noted that they used water-immiscible chloroform as the solvent.

We compared solutions in different solvents including water-immiscible chloroform and water-miscible tetrahydrofuran (THF) and different hydrophilic homopolymers.[139] It is interesting that the pore shape can be easily modulated. For chloroform systems, increasing the amount of homopolymer leads to decrease in interfacial tension; as a result, the pores of honeycomb films gradually change from near-spherical to ellipsoidal. For THF systems, the pores are always non-spherical, and large amounts of hydrophilic homopolymers are enriched in the pores.[139,171] The pore shape will be an important parameter for the use in templating and separation. Recently, Daly et al. proposed that the film structure is completely controlled by the properties of the water/solvent system, and the polymer is a spectator that only serves to capture the shape of the water droplet.[172] Although it should be noted that polymers especially amphiphilic polymers can change the interfacial tension and in turn affect the film structure, their results emphasized the importance of this interface. In fact, the interfacial tension is also a factor determining mono- or multilayer film structure except other factors such as solvent density, film thickness, polymer concentration, polymer structure, and addition of water to the solutions.[15,32,64,71,141,173,174]

### 3.2 Polymers with polar groups or blocks

It is accepted that solvent is a determining factor; however, the properties of polymer or other film-forming systems are also crucial to the formation of honeycomb films. PS without any polar groups can form ordered honeycomb films, as first proved by Han et al.[65] Non-polar polymers such as SIS can also form highly regular films under static conditions using high concentration solutions.[20,22,175] But it is well known that it is much easier to obtain honeycomb films by using polymers with polar end groups or blocks if the dynamic technique is adopted. The introduction of polar moieties shows great impact on film structures. For example, we found that the film changes from monolayer to multilayer by introducing a very short hydrophilic PHEMA block to a four-arm star PS or by using polymers with different hydrophilic end groups.[174] Polymers with polar moieties may self-assemble in organic solvent, changing solution viscosity,[64] and also segregate at the water/solution interface, inducing hierarchical structures. The hierarchical structures have received considerable attention. Protein microarrays can be fabricated based on honeycomb films prepared from PS terminated with carboxyl or amino groups.[62,176] During the BF process the condensation of water droplets allows reorientation of polymer chains by the interaction of the polar terminal groups with the water droplets so that porous films enriched with polar groups at the pore walls are obtained. Then proteins can be coupled to the site-specifically enriched carboxyl or amino groups, forming protein microarrays. Galeotti et al. also demonstrated that amino group is hydrophilic enough to produce PS honeycomb films in which the pores are effectively enriched with -$NH_2$ groups.[63]

When a linear amphiphilic block copolymer such as polystyrene-*block*-poly(2-hydroxyethyl methacrylate) (PS-*b*-PHEMA) is used for film formation, it serves as both a film-forming material and approximately a surfactant. We found that the latter role makes the hydrophilic block effectively aggregates toward water at the solution/water interface, generating films with a hierarchical structure. This hierarchical structure was confirmed by 3D reconstruction of confocal laser microscopy images after immobilizing 5-aminofluorescein to the hydroxyl groups (**Fig. 6a**).[54] The assembled hydroxyl groups can be easily converted into atom transfer radical polymerization (ATRP) initiator for preparing functional ordered films such as carbohydrate microarrays through site-specific modification (**Fig. 6b**).

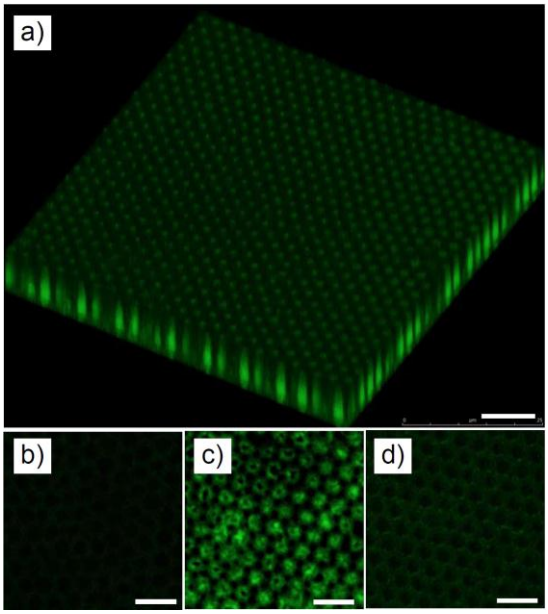


**Fig. 6** (a) 3D reconstruction of confocal laser scanning microscopy image of honeycomb films prepared from PS-*b*-PHEMA after staining with a fluorescent 5-AF. The scale bar is 10 μm. (b-d) Adsorption of fluorescence-tagged Con A on (b) PS-*b*-PHEMA and (c) glycosylated honeycomb films, and (d) adsorption of fluorescence-tagged peanut agglutinin (PNA) on a glycosylated honeycomb film. The scale bars are 5 μm. From ref. 54. Copyright 2010 American Chemical Society.

We developed a direct approach without post-modification to the fabrication of phenylboronic acid (PBA) arrays for biosensing. An amphiphilic block copolymer containing PBA pendants was synthesized by ATRP and subsequent chemical coupling for honeycomb film formation. The segregation of PBA pendants at the pore wall enables sensitive glucose sensing.[152] It can be achieved by two routes; one is visual detection through fluorescence quenching and the other is based on quartz crystal microbalance (QCM). In the former route, PBA can bond with Alizarin Red S. (ARS) that does not emit fluorescence itself, forming a PBA-ARS complex that is able to emit fluorescence. The recognition of saccharide such as glucose with BPA competes with the BPA-ARS complex, releasing ARS and quenching fluorescence (**Fig. 7a**). In the latter route, honeycomb films coated on a QCM chip can be directly applied to glucose sensing (**Fig. 7b**). We revealed that, compared with non-porous film, the enhanced sensing performance of honeycomb film is induced by not only the larger specific surface area but also the segregation of PBA pendants.

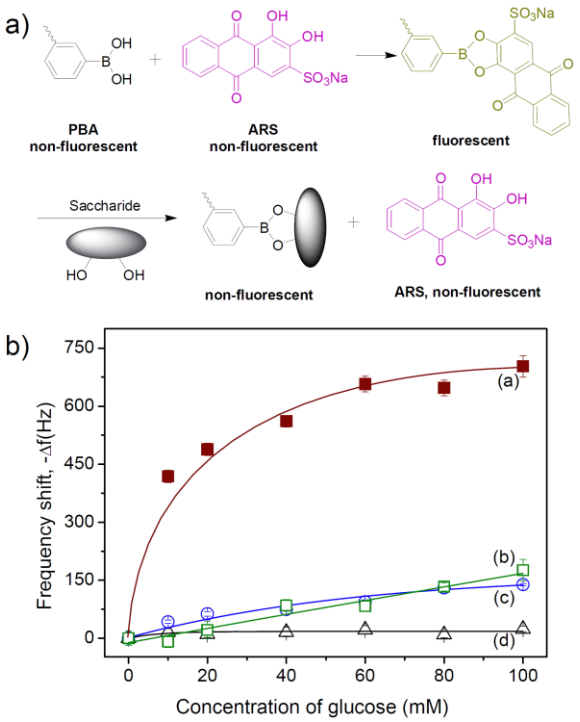


**Fig. 7** (a) Schematic illustration of the interaction between Alizarin Red S. (ARS), saccharide and phenylboronic acid (PBA). (b) QCM results of different films exposed to glucose solution. honeycomb films with PBA pendents (a) after being pre-wetted with ethanol and (b) without being pre-wetted, (c) dense films, (d) PS-*b*-PAA honeycomb films after being pre-wetted with ethanol. From ref. 152. Copyright 2011 American Chemical Society.

### 3.3 Blends containing polar homopolymers

It is well known that polymer blends may tend to form phase separated structures, which is different from block copolymers that usually undergo microphase separation because the blocks are chemically bonded. On one hand, the phase separation of blends may lead to honeycomb films with new structures. On the other hand, although the development of controlled/"living" radical polymerization enables facile synthesis of a great variety of block copolymers, blending a polymer with another polymer is still a simple and effective method to create "new" materials. A typical example is that reported by Han et al. who used the blends of PS and poly(2-vinyl pyridine) (P2VP).[177,178] They found that the hexagonal arrays of pores can be produced from the PS/P2VP blend only when the relative humidity is higher than a critical value (~30%). They observed water-induced reversible transition of surface morphologies. As shown in **Fig. 8**, island-like structure appears if the sample is dipped in water for 20 min, and the islands become larger after being immersed in water for 2 h; when the film is dried, the pores recover completely as the original topography.[177] This reversible morphology transition demonstrated that the P2VP-rich phase domains are inside the pores. The authors also showed the reversibility induced by other solvents.[178] Recently, Ge and Lu reported similar behavior for PS/poly(vinyl pyrrolidone) system; ordered films with controllable microstructures were used as replication templates.[144]



 

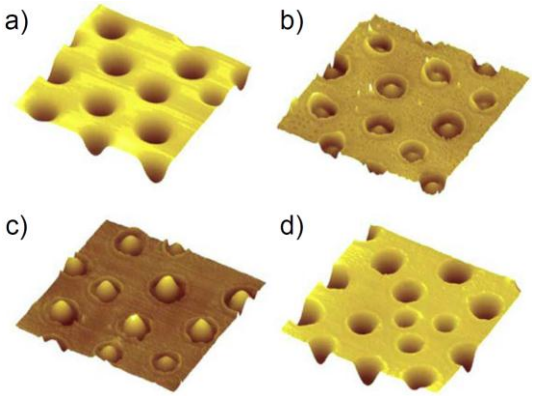


**Fig. 8** AFM images of PS/P2VP honeycomb films immersed in water at different time: (a) 0 min (in air), (b) 20 min, (c) 1 h, and (d) after drying. From ref. 177.

Poly(ethylene glycol) (PEG) is a well-known water-soluble polymer that is biocompatible. PEG with different molecular weight can be obtained commercially. Consequently, PS/PEG is another interesting blend system. Ohshima et al. made solutions of PS/PEG in toluene and found the enrichment of PEG as a ring around the pores, which was carefully characterized by gel permeation chromatography (GPC) analysis.[89] Interestingly, they observed some pores at the substrate side (aluminum Petri dish) (**Fig. 9**), which is different from the typical structure of honeycomb films. This unique structure is attributed by the authors to the higher density of PEG (1.11 g/cm$^3$) than those of PS (1.04 g/cm$^3$) and the solvent toluene (0.87 g/cm$^3$). The interfacial energy between the polymer solution and the substrate may also play an important role; however, more results are needed to support this hypothesis. For PS/PEG honeycomb films, we demonstrated the water-induced reversible morphology transition using AFM.[179]

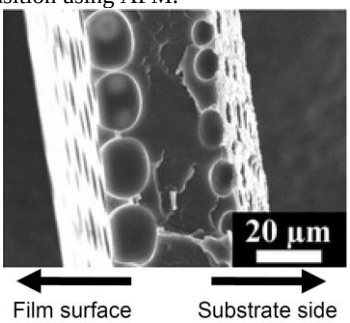


**Fig. 9** Cross-sectional SEM micrograph of PS/PEG200 (70/30, w/w) cast from 90 wt% toluene solution under a 3 L/min $N_2$ flow. From ref. 89. Copyright 2007 American Chemical Society.

Rodriguez-Hernandez group contributed some different but really interesting examples. Generally, hydrophilic homopolymers are used as additives for film formation; in contrast, they used hydrophobic fluorinated polymers.[34,90,180] For example, they prepared porous films from ternary blends of high-molecular-weight polystyrene, amphiphilic polystyrene-*block*-poly[poly(ethylene glycol) methyl ether methacrylate] (PS-*b*-PPEGMA), and poly(2,3,4,5,6-pentafluorostyrene) (P5FS$_{21}$). It was found by confocal micro-Raman spectroscopy that the hydrophilic PEG block enriches mainly in the pores whereas the hydrophobic fluorinated homopolymer phase separated at the top surface around the pores (**Fig. 10**). Thiolated glucose molecules were specifically attached to the P5FS$_{21}$ domains via a thiol-*para* fluorine "click" reaction, leading to selective modification of the surface outside the pores.[181] Subsequently, a specific lectin Concanavalin A (Con A) can be attached to the surface by conjugation with the glucose moieties (**Fig. 11**).[180,181]

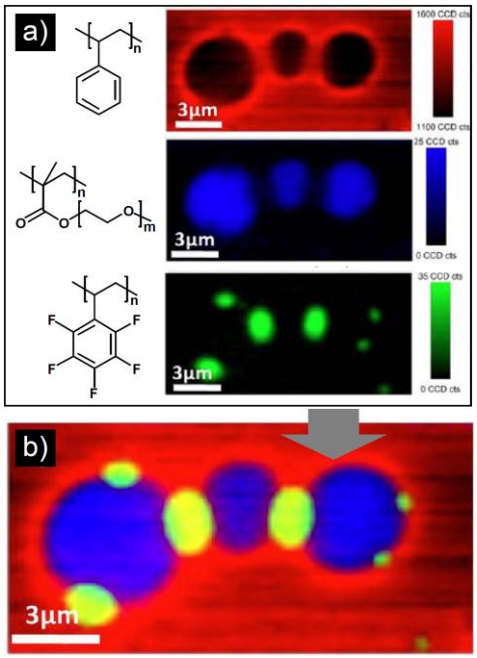


**Fig. 10** (a) Separate Raman maps of the components of the blend in the honeycomb films. Red regions represent the higher intensity for the 1012 cm$^{-1}$ associated with PS while the integrated intensities of the Raman peaks at 1663 cm$^{-1}$ for the P5FS$_{21}$ and 1735 cm$^{-1}$ associated with the P(PEGMA) are shown in a color green and blue color, respectively. (b) A typical Raman micrograph constructed by merging the maps of the three components for films prepared from the blend. From ref. 180. Copyright 2013 American Chemical Society.

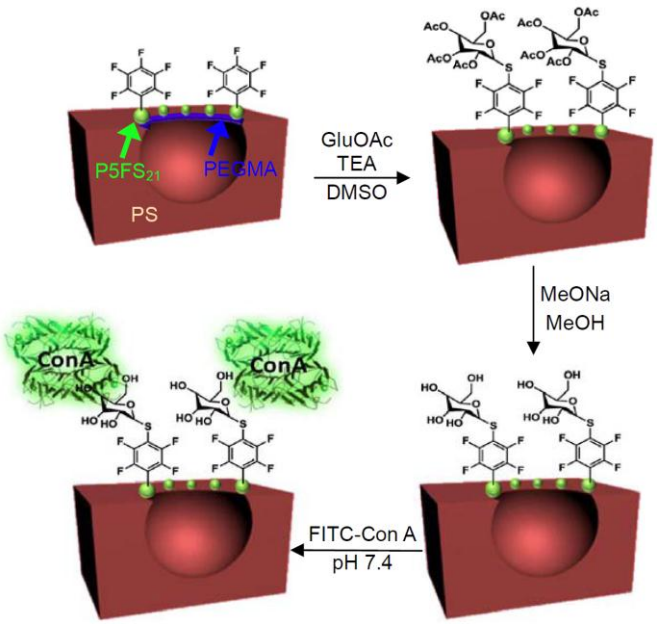


**Fig. 11** Schematic representation of the approach employed to incorporate glucose moieties and, subsequently, Con A onto the honeycomb films. From ref. 180. Copyright 2013 American Chemical Society.

### 3.4 Nanoparticles and nanogels

As early as 2004, Russell et al. reported honeycomb films where the pore walls are decorated with CdSe nanoparticles.[182] The

nanoparticles in the solution can enrich at the solution/water interface via self-assembly. Modification of the ligands attached to the nanoparticles opens a simple route to functionalize the surfaces of the spherical pores. Ji et al. dispersed silica nanoparticles suspension in absolute ethanol to PS solution in chloroform for honeycomb film formation.[107] They found that silica nanoparticles self-assemble at the pore walls, forming a hierarchical structure. It was proposed that the combination of Pickering emulsions and capillary flow in the BF method is responsible for this structure. They also demonstrated that particles with larger size help to achieve more regular honeycomb films as more energy is required to remove larger particles adsorbed at the interface.[113] Similarly, $Fe_3O_4$, Au, and Ag nanoparticles, poly[(*N*-isopropylacrylamide)-*co*-(acrylic acid)] microgels, and polystyrene particles can self-assemble at the interface to form hierarchical honeycomb films.[100,109,113]

Based on this strategy, we fabricated a functional honeycomb film with self-assembled enzyme nanogels at the pore walls for biocatalysis.[153] Horseradish peroxidase (HRP) is widely used as a component of clinical diagnostic kits and for immunoassays. We synthesized HRP nanogels that consist of almost one single HRP molecule as the core in each nanogel and a very thin crosslinked hydrophilic shell (**Fig. 12a**). This protected HRP can be dispersed in ethanol and then added to a PS solution for honeycomb film preparation. The pore walls are decorated with HRP nanogels, as revealed by confocal Raman spectroscopy imaging (**Fig. 12b**) and confocal laser scanning microscopy. Therefore, much more enzyme molecules are accessible to the substrate molecules in honeycomb films than in dense films prepared by casting or spin-coating. Furthermore, the films with HRP nanogels show robust catalysis reactivity compared with films with unprotected HRP because the HRP nanogels possess higher stability to external stimulus such as exposure to organic solvents. This one-step method can also be applied to the self-assembly of other biomacromolecules.

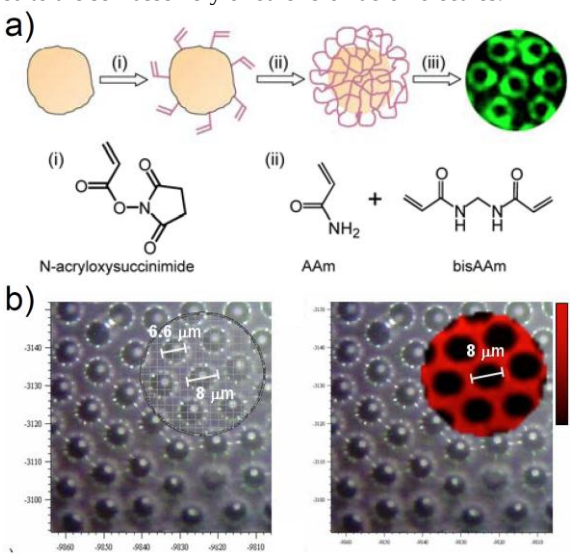


**Fig. 12** (a) Synthesis of HRP nanoparticles and preparation of HRP patterns. i) Vinyl groups were introduced to HRP molecule surface. ii) AAm and bisAAm were copolymerized on vinyl HRP to form a thin cross-linked shell. iii) HRP NPs were added to PS/chloroform solution to form honeycomb films. (b) (left) Optical image of honeycomb film containing HRP nanoparticles with a pore diameter of ~6.6 μm. (right) Confocal Raman spectroscopy image at Raman shift of 1003 $cm^{-1}$, which was stacked on the corresponding optical image. The scattering intensity increases with color changing from black to red. From ref. 153.

It is not always true (or necessary) that the pore walls would be enriched with nanoparticles. Recently, Saito et al. stabilized $Al_2O_3$ nanoparticles with mussel-inspired amphiphilic copolymers containing catechol moieties for honeycomb film preparation.[93] It was found that the polymer is mainly distributed around the pores and there were no $Al_2O_3$ nanoparticles at the pore edges. The films can be sintered to produce porous bulk $Al_2O_3$ films that are thermally and chemically stable.

### 3.5 Interfacial reactions

As mentioned above, polar groups and blocks, homopolymer additives, nanoparticles, and nanogels may self-assemble at the water/solution interface as these items are able to stabilize the water droplets. If substances that can react with water are used as additives, what film structure can we obtain? Zhao et al. added titanium tetraisopropoxide (TTIP) into PS solution in chloroform, and the solution was cast under a flow with a relative humidity of 83%.[108] Ordered films with the precursor of $TiO_2$, i.e., TTIP, were prepared. They found that honeycomb $TiO_2$ films can be obtained by calcination at 550 $^oC$ only after vapor phase hydrothermal treatment under a 100% relative humidity at 100 $^oC$, otherwise the honeycomb structure was completely destroyed as a result of the pyrolysis. They described that hydrolization products of TTIP that are hydrophilic can be accumulated at the water/solution interface. By the combination of the BF method and calcination at high temperature, homogeneous $TiO_2$ honeycomb films were also prepared from the solution of PS and titanium *n*-butoxide (TBT).[183] However, when TTIP or TBT was replaced by $TiCl_4$ that reacts with water violently, a totally different honeycomb film was formed.[184] Hydrolysis of $TiCl_4$ proceeds spontaneously at the water interface and even in the bulk of the water droplets, leading to honeycomb pores filled with hemispherical or mushroom-like $TiO_2$ microparticles. Similarly, bowl-like $SnO_2$ microparticles can be formed using $SnCl_4$ as the precursor.[185] Ordered hybrid or inorganic honeycomb films can be fabricated by this method through rational choice of precursors that react with water. It can also be considered as a novel strategy to synthesize microparticles.

### 3.6 Use of non-aqueous vapors

In the traditional BF method, aqueous vapor is always used to introduce water droplets as the self-assembling templates. Because water has relatively large surface tension, spherical pores are often generated in honeycomb films. Can non-aqueous vapor be used in the BF method? Zuo et al. investigated the self-assembly of a rod-coil diblock copolymer under a methanol gas flow. They achieved porous films and well-defined vesicles, which depend on the solution concentration.[186] They suggest that the methanol droplets are not as stable as water droplets because methanol is miscible with the solvent they used, resulting in coalescence of methanol droplets frequently. In fact, it may also relate to the interfacial tension. Xiong et al. prepared microspheres patterns, the "reverse" breath figures, by casting solution in toluene under a methanol environment.[187] Li and coworkers used a polydimethylsiloxane-*block*-polystyrene PDMS-*b*-PS solution in $CS_2$ to prepare honeycomb films under methanol atmosphere. In this elegant study, they obtained highly ordered honeycomb films with U-shaped cross-sectional structure and larger pore size than those templated by water droplets.[188] They also systematically compared films formed under methanol, ethanol, and water vapors.[29] Typical size and shape of the films are shown in **Fig. 13**. The differences were explained by the different physical properties of the vapors used, such as surface tension and evaporation enthalpy. Use of non-aqueous vapors may provide new



 

opportunities of creating honeycomb films with new structures or functions.

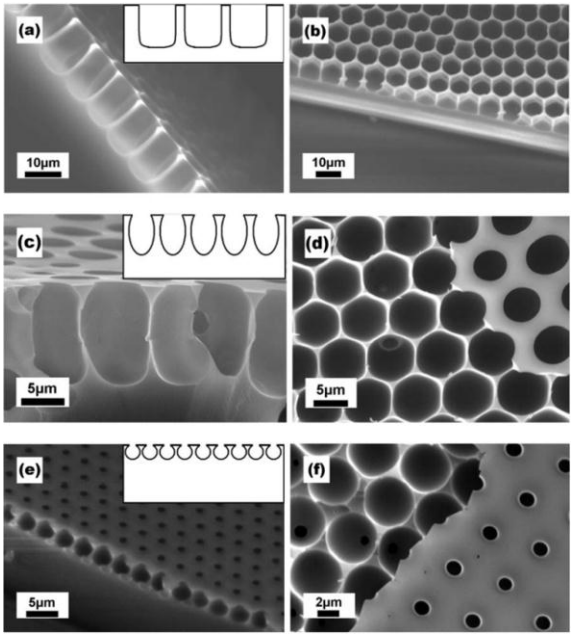


**Fig. 13** SEM images showing the shapes of pores in the polymer films prepared under different vapor atmospheres. Cross-section views of films produced in methanol, ethanol and water atmospheres are shown in (a), (c) and (e), respectively, and the contour lines of the section of the pores are shown in the insets. The corresponding top views of honeycomb arrays in the three films after peeling off the top layer are shown in the right column in (b), (d) and (f). From ref. 29.

### 3.7 Characterization of the interface chemistry

As mentioned above, the interface of water/solution is extremely important to the structures and functions of honeycomb films. However, it is difficult to characterize the chemistry at the interface. Here we would like to briefly summarize some useful techniques.

Fluorescence microscopy especially laser scanning confocal microscopy is a very effective technique to characterize the geometry[43,68,82] as well as chemistry[54,62,176] of the microstructures. Using this technique, the location and position of some known functional groups can be determined indirectly by coupling a fluorescent to these groups (**Fig. 6**).

AFM is also a widely used technique that is valid in both geometry and chemistry characterization, for example, based on the height and phase images, respectively.[34,177-179] One of the advantages of AFM lies in the fact that it is available to surface features ranging from a few nanometers to hundreds of micrometers with much higher resolution than other mapping or imaging techniques (**Fig. 8**). But it only gives the information of difference in surface chemistry in different domains, cannot tell us what groups or elements there exist.

Time-of-flight secondary-ion mass spectrometry (ToF-SIMS) provides the chemical composition of the extreme surface (depth < 3 nm) and includes imaging capabilities on the micrometer scale.[63] The generated ToF-SIMS images (e.g., 256 × 256 pixels) contain the full mass spectrum at every pixel, and thus it is possible to select images corresponding to atoms or molecular fragments of particular interest to get the information of their distribution.

Similar to ToF-SIMS, the mapping technique of Raman confocal microscopy enables fast and direct analysis of chemical groups and their distribution in the films (**Fig. 10 and 12**).[180,153] Furthermore, it can be utilized to analyze the distribution of functional groups in not only the xy plane but also the z direction, i.e., it can perform depth analysis.

## 4. Interfaces at the air side of honeycomb films

### 4.1 Cassie and Wenzel wetting states and the transition

Wettability of a solid surface is crucial in many practical applications. A direct expression of the wettability of a surface is the contact angle (CA) of a water drop placed on the surface (please note the difference in the terms of "water drop" and "water droplet" used in this article; here the former is artificially dropped onto film surface for CA measurement whereas the latter refers to those condensed from moist air during the breath figure process). It is well known that micro- and/or nano-structures are able to enhance the hydrophobicity or hydrophilicity. For example, one common strategy for superhydrophobic surface is to create pores or roughness that can capture air to prevent from being wetted by water, forming a so-called Cassie state.[189] In the Cassie state the water drop base rests only on the tips of the roughness elements; consequently, the base of the droplet is in composite contact with air and the top surface of honeycomb film in our case. The other extreme state of wetting is the Wenzel state in which the droplet wets the roughness elements completely and is in intimate contact with the solid substrate, i.e., the droplet fully wets the pores. On honeycomb films prepared from hydrophobic polymers, water droplet tends to form a Cassie state. The Cassie state is important to the construction of superhydrophobic surface, which will be discussed in the next subsection.

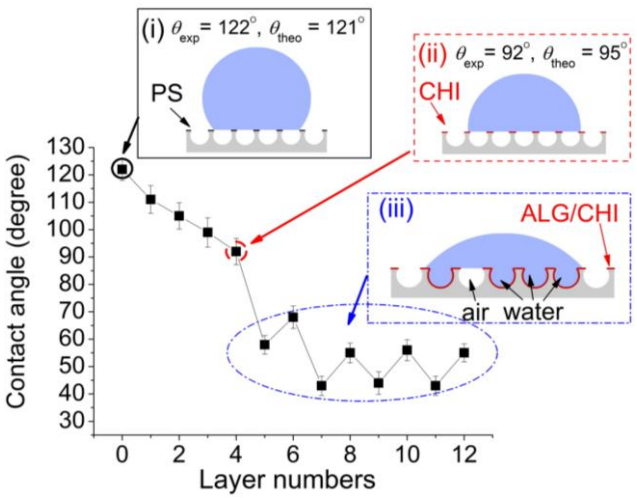


**Fig. 14** Contact angles on PS-*b*-PDMAEMA honeycomb films modified with certain number of (alginate/chitosan) layers. The film without modification is layer zero. (i) at layer zero, water droplet on the film surface (PS) is at the Cassie state, (ii) at layer four, water droplet on CHI-assembled surface is still at the Cassie state, and (iii) at layer five to twelve or more, water droplet is partly at the Wenzel state. From ref. 171.

It has been demonstrated both theoretically and experimentally that the Cassie-Wenzel wetting transition can take place in some conditions.[190] This transition has been clearly observed during the layer-by-layer (LBL) self-assembly process on a positively charged honeycomb film surface.[171] Such films were prepared by two routes, i.e., preparing films from quaternized PS-*b*-PDMAEMA or quaternizing PS-*b*-PDMAEMA films. Then polyelectrolytes such as alginate and chitosan can be alternately deposited on the film surface. Water CA on the original honeycomb film is as high as 122°, which is consistent with the theoretical value based on the Cassie and

Baxter's law, and decreases gradually with the LBL self-assembly of hydrophilic polyelectrolytes (**Fig. 14**). For films with the first four layers of polyelectrolytes, the water CA remains higher than 90°. As the polyelectrolytes assemble continuously, the CA decreases to below 90° and then exhibits a typical zigzag feature with the layer number because alginate is slightly more hydrophilic than chitosan. It should be noted that there is a sudden decrease from the fourth to the fifth layer. Results of QCM also support this sudden change, which is attributed to the Cassie-Wenzel transition at which the pores start to be wetted as a result of hydrophilization by polyelectrolytes. On the honeycomb films prepared from polycarbonate (PC) on stainless steel gauzes (**Fig. 5f**), Cassie-Wenzel wetting transition was also observed under an applied electrical field.[132]

The Cassie-Wenzel wetting transition is very useful in controlling functional self-assemblies. For example, filling microspheres into the pores is an easy way to form functional microarrays.[61] Transition from the Cassie state to the Wenzel state will help the filling process.[191,192] By controlling the wetting states, we achieved site-specific self-assembly of nanoparticles on/in honeycomb films (**Fig. 15**).[55] Silica nanoparticles that are negatively charged can selectively assemble on the external surface from its water dispersions at a Cassie state, or assemble across all surfaces of the film by pre-wetting the honeycomb film using ethanol to attain a Wenzel state. To assemble the nanoparticles only inside the pores, a layer of negatively charged PAA is introduced onto the external surface of the film at a Cassie state. This PAA layer can prevent the nanoparticles from assembling on the external surface based on the principle of like charges repel each other. Consequently, the nanoparticles selectively assemble inside or outside the pores. Recently, Rodriguez-Hernandez et al. achieved specific modification of the surface outside the pores through controlling the wetting state. Interestingly, they performed a thiol-*para* fluorine "click" reaction (**Fig. 11**) on a more hydrophobic film prepared from fluorinated copolymer.[181] It can be speculated that the Cassie-Wenzel transition will be the key to site-specific assemblies on the highly porous films.

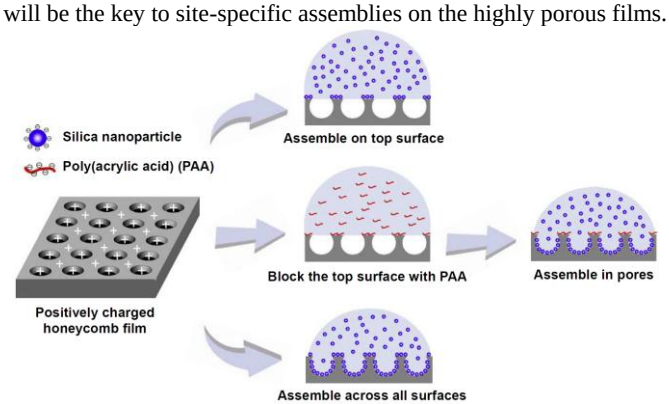


**Fig. 15** Site-specific assembly of negatively charged silica nanoparticles on positively charged honeycomb films. From ref. 55. Copyright 2010 American Chemical Society.

### 4.2 Superhydrophobic surfaces

A superhydrophobic surface usually has a CA larger than 150°.[193] Superhydrophobic surfaces have found applications in a variety of fields, such as self-cleaning surface and prevention of snow sticking. Formation of highly porous or rough structures is an effective and almost necessary strategy to prepare superhydrophobic surfaces. As we know, honeycomb film has a surface with porosity more than 50%.[171] Moreover, the top layer of honeycomb films can be very easily peeled off, exposing a pincushion structure with even higher porosity and larger roughness. Yabu et al. prepared highly ordered honeycomb films from a fluorinated copolymer.[150] They found that the corresponding flat film has a water CA about 117°, whereas the honeycomb film reaches 145°. After peeling off the top layer using adhesive tape, the pincushion-like structure possesses a CA as high as 170° (**Fig. 16a**). In addition, this surface is also lipophobic, on which the CA of benzene can reach 135°. If the pore size of the honeycomb films further decreases to about 300 nm, films even with the top layer become superhydrophobic and transparent (**Fig. 16b**).[151] Superhydrophobic surface can also be obtained by using a specially designed waxy-dendron-grafted polymer to form honeycomb film with pincushion-like structure.[194] It is obvious that this BF-based method has a lot of advantages, for example, it is a low-cost fabrication process with low energy consumption and can be applied to various hydrophobic polymers.

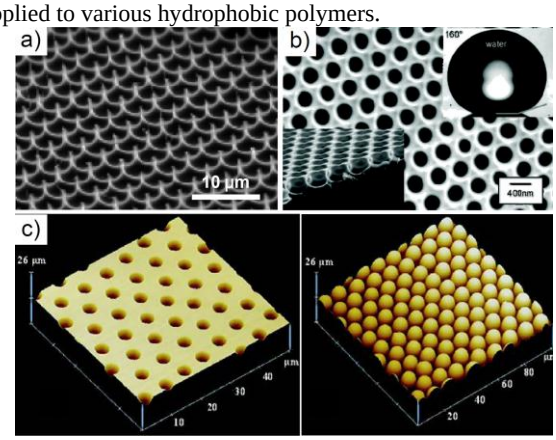


**Fig. 16** (a) SEM image of honeycomb film with a typical pincushion structure. From ref. 150. (b) SEM image of a 300-nm-sized honeycomb film (top surface and cross section) and the water contact angle on this film. From ref. 151. (c) AFM images of silicone pillars (GE Silicons RTV 615 silicon rubber). Honeycomb film before templating step (left) and the templated pillars (right). From ref. 195. Copyright American Chemical Society.

For honeycomb films prepared from non-fluorinated polymers, superhydrophobic surfaces can be constructed through simple post-modification. For example, Badyal et al. prepared superhydrophobic polybutadiene film by $CF_4$ plasmachemical fluorination.[26] This treatment causes crosslinking and surface texturing, leading to hierarchical surfaces with multiscale roughness. The surfaces show high water CA of more than 170° and low CA hysteresis.

The superhydrophobic characteristic of honeycomb film surface can be transferred to other materials. One simple approach is using these ordered pores as templates to fabricate the analogous array of pillars, i.e., inverse pores (**Fig. 16c**).[195] Such surface with protuberances exhibits greatly enhanced hydrophobicity.

### 4.3 Hydrophilic surfaces

If the films are prepared from hydrophilic polymers, the roughness induced by the honeycomb structure may enhance the hydrophilicity according to the Wenzel's theory. Based on the mechanism of the BF method, solvents that are highly volatile and non-polar or low-polar such as $CS_2$ and chloroform are often used. For this reason, non-polar or amphiphilic polymers with short hydrophilic block are generally used in the BF method. Therefore, in contrast to hydrophobic or superhydrophobic surfaces, hydrophilic honeycomb films are scarcely reported. One typical example is honeycomb films prepared from polystryene-*block*-poly(acrylic acid) PS-*b*-PAA which show a highly hydrophilic surface at high pH values. Hu et al. cast PS-*b*-PAA solution in THF on different substrates under a humid air flow and studied the effects of a series of factors on the film formation.[50] It was found that water drop placed on the surfaces



 

of the honeycomb films can change its CA with time by interacting with the hydrophilic PAA blocks and inducing the segregation toward water/film interface. Interestingly, if water at pH 10 is used for CA measurement, the time CA changes decreases remarkably. In other words, the ionized PAA together with the honeycomb structure enables a nearly superhydrophilic surface with a zero water CA. In fact, there may exist a Cassie-Wenzel transition. Karthaus et al. used poly[styrene-*co*-(maleic anhydride)] PS-*co*-PMA for crosslinked honeycomb films that are thermally stable and solvent resistant. Interestingly, the crosslinking reaction will produce a carboxyl group, which changes the hydrophobic surface to hydrophilic.[47] Li et al. prepared honeycomb films from commercially available polystyrene-*block*-polybutadiene-*block*-polystyrene (SBS).[175] Photo-chemical crosslinking was carried out using deep UV light with a wavelength of 254 nm. This modification leads to improved solvent and thermal stability. Besides, the modification also changes the surface wettability from hydrophobic to hydrophilic. They contended that this change is enhanced by the micro-patterned structure. The hydrophilized honeycomb films are useful in cell culture.

### 4.4 Adhesive surfaces

The highly porous feature of honeycomb films makes the surfaces water-adhesive. Heng et al. designed an adhesive surface based on the BF method.[196] They found that the negative pressure produced by the sealed air in the pores is the crucial factor for the adhesive surface (**Fig. 17**). Moreover, larger volume of air sealed between water and the substrate results in lower adhesion.

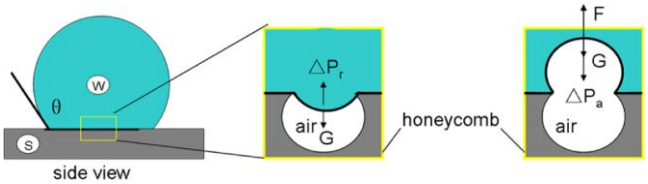


**Fig. 17** Schematic illustrations of the interfaces between water and a single honeycomb structural pore and the volume change of the sealed air in one PS pore upon the action of external force. Capillary adhesion arises when a water droplet sitting on the pore is gradually drawn upward because the convex air/liquid interface produces an inward pressure ΔP. W represents water droplet, and S represents solid film. From ref. 196. Copyright 2013 American Chemical Society.

Honeycomb films can also be used as scaffolds for cell adhesion and culture. Using honeycomb films as cell culture scaffolds starts early. In 1999, Nishikawa, Shimomura, and coworkers reported the adhesion of bovine aorta endothelial cells to honeycomb films prepared from different polymers, such as amphiphilic copolymers containing lactose moieties or carboxyl groups and polyion complex containing dextran sulfate or heparin.[197] They found that the cells adhere to all the four honeycomb films; however, on unpatterned heparin-containing surface the cell density is very low. Consequently, they concluded that the honeycomb structure works as an adhesive site for cells.[147,197] Stenzel et al. also demonstrated that the unique surface topography of honeycomb films show obvious influences on cell adhesion and proliferation.[198] On the flat film prepared from a home-made block copolymer with polypyrrole cell density is almost zero. Nevertheless, the cells can adhere to and proliferate on the corresponding honeycomb films. Moreover, the adhesion depends on the pore size;[198,199] on films with pores larger than 1 μm, the cell density is comparable to that on cell culture PS flat film. Another interesting example is the selective adhesion of bacteria, which is based on site-specific modification of the pores by polypeptide sequences on honeycomb films. The films were fabricated from the blends of PS and PS-*b*-PAA in which the PAA block segregated at the interface of water droplets and solution.[200] Recently, Yabu and coworkers proposed that hard honeycomb films are better for cell adhesion than soft films.[201] Cell adhesion on honeycomb films with mechanically deformed structures[146] or those prepared from biodegradable materials[75-77,202] has also been widely investigated.

### 4.5 Stimuli-responsive surfaces

Stimuli-responsive surfaces have received considerable attention because of their applications, for example, in drug and gene delivery, sensing, wettability switching, and so on, under different external stimulus such as temperature, solvent, pH, light, or mechanical stress.[203,204] Based on honeycomb films, some interesting results that are different from flat films have been reported. Stenzel et al. used a block copolymer polystyrene-*block*-poly(*N*-isopropyl acrylamide) PS-*b*-PNIPAM for the preparation of thin dense film, honeycomb films, and the corresponding pincushion-like films after removing the top surfaces.[205] They found that the thin dense film and pincushion-like film show obvious thermo-responsive property whereas the honeycomb film doesn't. It is because PNIPAM block that is thermo-responsive mainly segregates at the interface of water/solution, forming a hydrophobic top surface and hydrophilic pores (see Section 3 for more details). Yabu et al. observed similar phenomena from the honeycomb films prepared from the blend of PS and a copolymer containing PNIPAM; only the pincushion-like films show the response.[206]

Stenzel and coworkers also fabricated thermo-responsive honeycomb films by grafting PNIPAM from PS-*co*-PHEMA film surface.[16] The grafted surface is slightly different from that directly prepared from PS-*b*-PNIPAM. The grafting mainly takes place in the pores; however, it also results in a modified surface. Therefore, the honeycomb films grafted with PNIPAM also display switchable hydrophilic/hydrophobic characteristics. If the copolymer of NIPAM and *N*-acryloyl glucosamine is grafted from the honeycomb film surface, it shows selective recognition of Con A. Below the lower critical solution temperature (LCST) of the surface, the conjugation is switched off, while above the LCST the surface grafted with glucose moieties can strongly bind to Con A.[207]

pH-sensitive honeycomb films have been investigated by Save and Billon.[208,209] They presented an interesting hierarchical PS-*b*-P4VP surface composed of pores at the micrometer scale and phase separated structures at the nanometer scale. It was proved that the pincushion-like structure can enhance the response to pH; the contact angle variation is 20° between pH 9 and pH 3 on the honeycomb film but increases to 72° on the pincushion-like surface (**Fig. 18**).[208] Recently, they synthesized polystyrene-*block*-poly(ethoxy ethyl acrylate) PS-*b*-PEEA diblock copolymer with high molar mass of PEEA using Cu(0)-mediated controlled radical polymerization.[209] This polymer was used for preparing honeycomb film by the BF method followed by thermolysis at 90 °C. Before thermolysis, the PS-*b*-PEEA film exhibits a superhydrophobic surface with a water CA of 155° after removing the top surface layer. After thermolysis, the resulting PS-*b*-PAA honeycomb film shows obvious pH-responsive characteristics with a CA variation of 65° between pH 3 and pH 10. However, differing from the above-mentioned samples, the pincushion-like surface shows smaller CA variation (~30°) because the segregation of hydrophilic PEEA leads to too much PAA blocks at the surface of pincushion-like structure. Considering this hierarchical structure with segregated carboxyl groups, it may provide not only a pH-responsive surface but also a platform for functional films through site-specific post-modification. In summary, the responsive behaviors on honeycomb film surface are dependent on the unique structure, which makes it possible to design new smart surfaces.

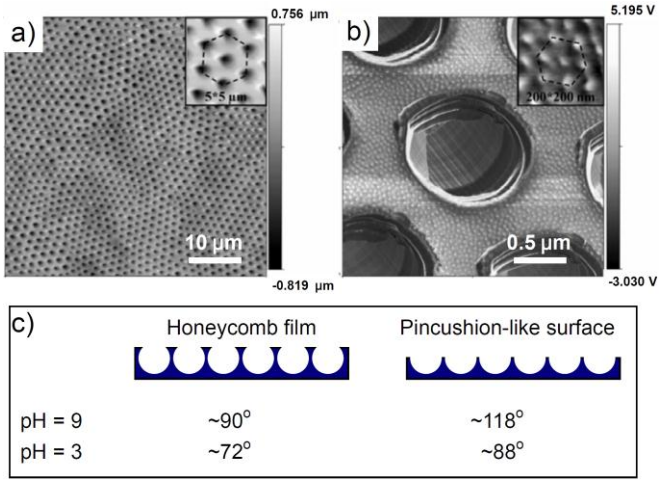


**Fig. 18** (a,b) AFM images of PS-*b*-P4VP honeycomb film recorded in topographic mode (a) and phase mode (b). (c) Water contact angles on the honeycomb film and pincushion-like surface measured at pH 3 and 9. From ref. 208.

## 5. Conclusions and perspectives

Since the discovery by Widawski, Francois and coworkers in 1994, the BF method has shown great potentials in chemistry and materials science as a dynamic templating technique for ordered films with micro- and nano-structures. The use of condensed water droplets as templates enables a microfabrication process of efficient, low-cost, simple, and sustainable. The water droplets also induce orientation of polar groups and blocks, water-soluble homopolymers, nanoparticles and nanogels at the interface of water droplet and solution. Consequently, it is easy to form patterned films with hierarchical structures via a one-step process. Furthermore, different substrates may lead to films with various patterns and structures such as through pores, hexagonal or square arrays, and complex 3D architectures. In addition, the highly porous honeycomb films, which can be prepared from a great variety of materials such as polymers, small molecules, and stabilized nanoparticles, show interesting wettability such as Cassie-Wenzel transition and enhanced/adjustable stimuli-responses. All the above-mentioned characteristics endow the BF method with great advantages over other traditional patterning techniques.

To push forward the development of the BF method, great efforts must be made in both fundamental and applied aspects. Although the principle of the BF method looks very simple, the exact mechanism is still not known in detail. For example, tiny changes in polymer structure may result in obviously diverse structures in the honeycomb films; the effects of some operation factors such as solvents and polymer concentration vary for different film-forming systems. Understanding the exact mechanism with more experimental results will be helpful in fabricating honeycomb films in a more controllable way. The interfacial interactions between water droplets and the solution are believed to play a key role.

The honeycomb films have shown potential applications as optical materials, separation membranes, superhydrophobic coatings, sensing films, etc. Formation of honeycomb films toward practical applications requires rational design of film-forming materials, sophisticated but robust structures including sub-structures, and high performances. Modulation of the multiple interfacial behaviors will provide an effective approach to convenient control over honeycomb films with high reproducibility, high ordering, and hierarchical structures. For example, controlled self-assembly at an ice/air interface is able to generate highly ordered honeycomb membranes with through pores for size-selective separation, which will be interested in the frontiers of chemistry, materials, and biology.

## Acknowledgements

Financial support from the National Natural Science Foundation of China (21374100, 51173161, and 50803053), the Zhejiang Provincial Natural Science Foundation of China (Y4110076) and the State Key Laboratory of Materials-Oriented Chemical Engineering (KL13-11) is gratefully acknowledged. Ling-Shu Wan would like to thank all his current and past students, particularly Dr. Bei-Bei Ke, Jing Jin, Xiao-Kai Li, Lu-Yao Zhang, Jie Lv, Wen-Xu Zhang, Peng-Cheng Chen, Qing-Lian Li, and Xuan Yang.

## Notes and references

MOE Key Laboratory of Macromolecular Synthesis and Functionalization, Department of Polymer Science and Engineering, Zhejiang University, Hangzhou 310027, China.
E-mail: lswan@zju.edu.cn

1 Rayleigh, *Nature*, 1911, **86**, 416.
2 J. Aitken, *Nature*, 1913, **90**, 619.
3 G. Widawski, M. Rawiso and B. Francois, *Nature*, 1994, **369**, 387.
4 M. Srinivasarao, D. Collings, A. Philips and S. Patel, *Science*, 2001, **292**, 79.
5 N. Maruyama, T. Koito, J. Nishida, T. Sawadaishi, X. Cieren, K. Ijiro, O. Karthaus and M. Shimomura, *Thin Solid Films*, 1998, **327**, 854.
6 M. H. Stenzel, *Aust. J. Chem.*, 2002, **55**, 239.
7 U. H. F. Bunz, *Adv. Mater.*, 2006, **18**, 973.
8 M. H. Stenzel, C. Barner-Kowollik and T. P. Davis, *J. Polym. Sci. Part A: Polym. Chem.*, 2006, **44**, 2363.
9 H. M. Ma and J. C. Hao, *Chem. Soc. Rev.*, 2011, **40**, 5457.
10 X. P. Xiong, M. F. Lin and W. W. Zou, *Curr. Org. Chem.*, 2011, **15**, 3706.
11 M. Hernandez-Guerrero and M. H. Stenzel, *Polym. Chem.*, 2012, **3**, 563.
12 P. Escale, L. Rubatat, L. Billon and M. Save, *Eur. Polym. J.*, 2012, **48**, 1001.
13 L. J. Xue, J. L. Zhang and Y. C. Han, *Prog. Polym. Sci.*, 2012, **37**, 564.
14 H. Bai, C. Du, A. Zhang and L. Li, *Angew. Chem. Int. Ed.*, 2013, **52**, 12240.
15 A. Bolognesi, C. Mercogliano, S. Yunus, M. Civardi, D. Comoretto and A. Turturro, *Langmuir*, 2005, **21**, 3480.
16 M. Hernandez-Guerrero, E. Min, C. Barner-Kowollik, A. H. E. Muller and M. H. Stenzel, *J. Mater. Chem.*, 2008, **18**, 4718.
17 A. Gugliuzza, M. C. Aceto, F. Macedonio and E. Drioli, *J. Phys. Chem. B*, 2008, **112**, 10483.
18 L. Li, Y. W. Zhong, J. Li, C. K. Chen, A. J. Zhang, J. Xu and Z. Ma, *J. Mater. Chem.*, 2009, **19**, 7222.
19 L. Li, J. A. Li, Y. W. Zhong, C. K. Chen, Y. Ben, J. L. Gong and Z. Ma, *J. Mater. Chem.*, 2010, **20**, 5446.
20 L. Li, Y. W. Zhong, J. L. Gong, J. A. Li, C. K. Chen, B. R. Zeng and Z. Ma, *Soft Matter*, 2011, **7**, 546.
21 J. Li, Q. L. Zhao, J. Z. Chen, L. Li, J. Huang, Z. Ma and Y. W. Zhong, *Polym. Chem.*, 2010, **1**, 164.
22 L. Li, Y. W. Zhong, J. L. Gong, J. A. Li, J. Huang and Z. Ma, *J. Colloid Interf. Sci.*, 2011, **354**, 758.



 

23 J. Z. Chen, X. Z. Yan, Q. L. Zhao, L. Li and F. H. Huang, *Polym. Chem.*, 2012, **3**, 458.
24 Z. Zhang, X. J. Hao, P. A. Gurr, A. Blencowe, T. C. Hughes and G. G. Qiao, *Aust. J. Chem.*, 2012, **65**, 1186.
25 J. Y. Ding, J. L. Gong, H. Bai, L. Li, Y. W. Zhong, Z. Ma and V. Svrcek, *J. Colloid Interf. Sci.*, 2012, **380**, 99.
26 P. S. Brown, E. L. Talbot, T. J. Wood, C. D. Bain and J. P. S. Badyal, *Langmuir*, 2012, **28**, 13712.
27 Y. Xue, H. C. Lu, Q. L. Zhao, J. Huang, S. G. Xu, S. K. Cao and Z. Ma, *Polym. Chem.*, 2013, **4**, 307.
28 Z. Zhang, T. C. Hughes, P. A. Gurr, A. Blencowe, H. Uddin, X. J. Hao and G. G. Qiao, *Polymer*, 2013, **54**, 4446.
29 J. Y. Ding, A. J. Zhang, H. Bai, L. Li, J. Li and Z. Ma, *Soft Matter*, 2013, **9**, 506.
30 M. S. Park and J. K. Kim, *Langmuir*, 2004, **20**, 5347.
31 M. S. Park and J. K. Kim, *Langmuir*, 2005, **21**, 11404.
32 M. S. Park, W. Joo and J. K. Kim, *Langmuir*, 2006, **22**, 4594.
33 W. Madej, A. Budkowski, J. Raczkowska and J. Rysz, *Langmuir*, 2008, **24**, 3517.
34 A. Munoz-Bonilla, E. Ibarboure, E. Papon and J. Rodriguez-Hernandez, *Langmuir*, 2009, **25**, 6493.
35 A. Munoz-Bonilla, E. Ibarboure, V. Bordege, M. Fernandez-Garcia and J. Rodriguez-Hernandez, *Langmuir*, 2010, **26**, 8552.
36 J. Poly, E. Ibarboure, J. F. Le Meins, J. Rodriguez-Hernandez, D. Taton and E. Papon, *Langmuir*, 2011, **27**, 4290.
37 H. T. Ham, I. J. Chung, Y. S. Choi, S. H. Lee and S. O. Kim, *J. Phys. Chem. B*, 2006, **110**, 13959.
38 J. Mansouri, E. Yapit and V. Chen, *J. Membr. Sci.*, 2013, **444**, 237.
39 W. X. Zhang, L. S. Wan, X. L. Meng, J. W. Li, B. B. Ke, P. C. Chen and Z. K. Xu, *Soft Matter*, 2011, **7**, 4221.
40 Y. Y. Ma, J. Liang, H. Sun, L. X. Wu, Y. Q. Dang and Y. Q. Wu, *Chem.-Eur. J.*, 2012, **18**, 526.
41 J. Liang, Y. Y. Ma, H. Sun, W. Li and L. X. Wu, *J. Colloid Interf. Sci.*, 2013, **409**, 80.
42 T. Nishikawa, J. Nishida, R. Ookura, S. I. Nishimura, V. Scheumann, M. Zizlsperger, R. Lawall, W. Knoll and M. Shimomura, *Langmuir*, 2000, **16**, 1337.
43 C. Barner-Kowollik, H. Dalton, T. P. Davis and M. H. Stenzel, *Angew. Chem.-Int. Ed.*, 2003, **42**, 3664.
44 Z. Zhang, T. C. Hughes, P. A. Gurr, A. Blencowe, X. Hao and G. G. Qiao, *Adv. Mater.*, 2012, **24**, 4327.
45 M. H. Stenzel, T. P. Davis and A. G. Fane, *J. Mater. Chem.*, 2003, **13**, 2090.
46 L. A. Connal, R. Vestberg, P. A. Gurr, C. J. Hawker and G. G. Qiao, *Langmuir*, 2008, **24**, 556.
47 T. Kabuto, Y. Hashimoto and O. Karthaus, *Adv. Funct. Mater.*, 2007, **17**, 3569.
48 L. Li, Y. W. Zhong, C. Y. Ma, J. Li, C. K. Chen, A. J. Zhang, D. L. Tang, S. Y. Xie and Z. Ma, *Chem. Mater.*, 2009, **21**, 4977.
49 C. Y. Ma, Y. W. Zhong, J. Li, C. K. Chen, J. L. Gong, S. Y. Xie, L. Li and Z. Ma, *Chem. Mater.*, 2010, **22**, 2367.
50 C. Y. Wang, Y. D. Mao, D. Y. Wang, Q. S. Qu, G. J. Yang and X. Y. Hu, *J. Mater. Chem.*, 2008, **18**, 683.
51 A. Bolognesi, F. Galeotti, U. Giovanella, F. Bertini and S. Yunus, *Langmuir*, 2009, **25**, 5333.
52 P. Escale, S. R. S. Ting, A. Khoukh, L. Rubatat, M. Save, M. H. Stenzel and L. Billon, *Macromolecules*, 2011, **44**, 5911.
53 P. Escale, M. Save, A. Lapp, L. Rubatat and L. Billon, *Soft Matter*, 2010, **6**, 3202.
54 B. B. Ke, L. S. Wan and Z. K. Xu, *Langmuir*, 2010, **26**, 8946.
55 B. B. Ke, L. S. Wan, P. C. Chen, L. Y. Zhang and Z. K. Xu, *Langmuir*, 2010, **26**, 15982.
56 M. Kojima, T. Nakanishi, Y. Hirai, H. Yabu and M. Shimomura, *Chem. Commun.*, 2010, **46**, 3970.
57 K. H. Wong, M. H. Stenzel, S. Duvall and F. Ladouceur, *Chem. Mater.*, 2010, **22**, 1878.
58 T. Nakanishi, Y. Hirai, M. Kojima, H. Yabu and M. Shimomura, *J. Mater. Chem.*, 2010, **20**, 6741.
59 X. W. Zhu and M. H. Liu, *Langmuir*, 2011, **27**, 12844.
60 B. Zhao, C. X. Li, Y. Lu, X. D. Wang, Z. L. Liu and B. H. Zhang, *Polymer*, 2005, **46**, 9508.
61 M. H. Lu and Y. Zhang, *Adv. Mater.*, 2006, **18**, 3094.
62 Y. Zhang and C. Wang, *Adv. Mater.*, 2007, **19**, 913.
63 F. Galeotti, V. Calabrese, M. Cavazzini, S. Quici, C. Poleunis, S. Yunus and A. Bolognesi, *Chem. Mater.*, 2010, **22**, 2764.
64 L. Billon, M. Manguian, V. Pellerin, M. Joubert, O. Eterradossi and H. Garay, *Macromolecules*, 2009, **42**, 345.
65 J. Peng, Y. C. Han, Y. M. Yang and B. Y. Li, *Polymer*, 2004, **45**, 447.
66 Y. Xu, B. K. Zhu and Y. Y. Xu, *Polymer*, 2005, **46**, 713.
67 H. Y. Ma, Y. Tian and X. L. Wang, *Polymer*, 2011, **52**, 489.
68 C. H. Liu, C. Gao and D. Y. Yan, *Angew. Chem.-Int. Ed.*, 2007, **46**, 4128.
69 R. R. Hu, J. W. Y. Lam, M. Li, H. Q. Deng, J. Li and B. Z. Tang, *J. Polym. Sci. Part A: Polym. Chem.*, 2013, **51**, 4752.
70 W. Y. Dong, Y. F. Zhou, D. Y. Yan, Y. Y. Mai, L. He and C. Y. Jin, *Langmuir*, 2009, **25**, 173.
71 H. Ejima, T. Iwata and N. Yoshie, *Macromolecules*, 2008, **41**, 9846.
72 A. V. Vivek, K. Babu and R. Dhamodharan, *Macromolecules*, 2009, **42**, 2300.
73 O. C. J. Andren, M. V. Walter, T. Yang, A. Hult and M. Malkoch, *Macromolecules*, 2013, **46**, 3726.
74 B. B. Ke, L. S. Wan, W. X. Zhang and Z. K. Xu, *Polymer*, 2010, **51**, 2168.
75 Y. D. Zhu, R. L. Sheng, T. Luo, H. Li, J. J. Sun, S. D. Chen, W. Y. Sun and A. M. Cao, *ACS Appl. Mater. Interfaces*, 2011, **3**, 2487.
76 X. H. Wu and S. F. Wang, *ACS Appl. Mater. Interfaces*, 2012, **4**, 4966.
77 Y. Fukuhira, E. Kitazono, T. Hayashi, H. Kaneko, M. Tanaka, M. Shimomura and Y. Sumi, *Biomaterials*, 2006, **27**, 1797.
78 M. C. Du, P. L. Zhu, X. H. Yan, Y. Su, W. X. Song and J. B. Li, *Chem.-Eur. J.*, 2011, **17**, 4238.
79 B. H. Zhao, J. Zhang, X. D. Wang and C. X. Li, *J. Mater. Chem.*, 2006, **16**, 509.
80 H. H. Tsai, Z. H. Xu, R. K. Pai, L. Y. Wang, A. M. Dattelbaum, A. P. Shreve, H. L. Wang and M. Cotlet, *Chem. Mater.*, 2011, **23**, 759.
81 U. Stalmach, B. de Boer, C. Videlot, P. F. van Hutten and G. Hadziioannou, *J. Am. Chem. Soc.*, 2000, **122**, 5464.
82 B. Erdogan, L. L. Song, J. N. Wilson, J. O. Park, M. Srinivasarao and U. H. F. Bunz, *J. Am. Chem. Soc.*, 2004, **126**, 3678.
83 A. Bolognesi, F. Galeotti, J. Moreau, U. Giovanella, W. Porzio, G. Scavia and F. Bertini, *J. Mater. Chem.*, 2010, **20**, 1483.

84 Y. C. Chiu, C. C. Kuo, C. J. Lin and W. C. Chen, *Soft Matter*, 2011, **7**, 9350.
85 Y. Hirai, H. Yabu, Y. Matsuo, K. Ijiro and M. Shimomura, *Chem. Commun.*, 2010, **46**, 2298.
86 M. H. Stenzel-Rosenbaum, T. P. Davis, A. G. Fane and V. Chen, *Angew. Chem.-Int. Ed.*, 2001, **40**, 3428.
87 Y. Hirai, H. Yabu, Y. Matsuo, K. Ijiro and M. Shimomura, *J. Mater. Chem.*, 2010, **20**, 10804.
88 Y. Nakamichi, Y. Hirai, H. Yabu and M. Shimomura, *J. Mater. Chem.*, 2011, **21**, 3884.
89 J.-K. Kim, K. Taki and M. Ohshima, *Langmuir*, 2007, **23**, 12397.
90 A. S. de Leon, A. del Campo, M. Fernandez-Garcia, J. Rodriguez-Hernandez and A. Munoz-Bonilla, *Langmuir*, 2012, **28**, 9778.
91 J. Wang, C. F. Wang, H. X. Shen and S. Chen, *Chem. Commun.*, 2010, **46**, 7376.
92 H. M. Ma, J. W. Cui, A. X. Song and J. C. Hao, *Chem. Commun.*, 2011, **47**, 1154.
93 Y. Saito, M. Shimomura and H. Yabu, *Chem. Commun.*, 2013, **49**, 6081.
94 D. Fan, X. Jia, P. Tang, J. Hao and T. Liu, *Angew. Chem. Int. Ed.*, 2007, **46**, 3342.
95 S. H. Lee, H. W. Kim, J. O. Hwang, W. J. Lee, J. Kwon, C. W. Bielawski, R. S. Ruoff and S. O. Kim, *Angew. Chem.-Int. Ed.*, 2010, **49**, 10084.
96 S. Y. Yin, Y. Y. Zhang, J. H. Kong, C. J. Zou, C. M. Li, X. H. Lu, J. Ma, F. Y. C. Boey and X. D. Chen, *ACS Nano*, 2011, **5**, 3831.
97 N. Wakamatsu, H. Takamori, T. Fujigaya and N. Nakashima, *Adv. Funct. Mater.*, 2009, **19**, 311.
98 S. Y. Yin, Y. Goldovsky, M. Herzberg, L. Liu, H. Sun, Y. Y. Zhang, F. B. Meng, X. B. Cao, D. D. Sun, H. Y. Chen, A. Kushmaro and X. D. Chen, *Adv. Funct. Mater.*, 2013, **23**, 2972.
99 H. M. Ma and J. C. Hao, *Chem.-Eur. J.*, 2010, **16**, 655.
100 H. M. Ma, J. W. Cui, J. F. Chen and J. C. Hao, *Chem.-Eur. J.*, 2011, **17**, 655.
101 Y. Sakatani, C. Boissiere, D. Grosso, L. Nicole, G. Soler-Illia and C. Sanchez, *Chem. Mater.*, 2008, **20**, 1049.
102 H. T. Lord, J. F. Quinn, S. D. Angus, M. R. Whittaker, M. H. Stenzel and T. P. Davis, *J. Mater. Chem.*, 2003, **13**, 2819.
103 L. A. Connal, P. A. Gurr, G. G. Qiao and D. H. Solomon, *J. Mater. Chem.*, 2005, **15**, 1286.
104 H. Sun, H. L. Li, W. F. Bu, M. Xu and L. X. Wu, *J. Phys. Chem. B*, 2006, **110**, 24847.
105 H. Sun, W. Li, L. Wollenberg, B. Li, L. X. Wu, F. Y. Li and L. Xu, *J. Phys. Chem. B*, 2009, **113**, 14674.
106 J. Li, J. Peng, W. H. Huang, Y. Wu, J. Fu, Y. Cong, L. J. Xue and Y. C. Han, *Langmuir*, 2005, **21**, 2017.
107 W. Sun, J. Ji and J. C. Shen, *Langmuir*, 2008, **24**, 11338.
108 H. J. Zhao, Y. M. Shen, S. Q. Zhang and H. M. Zhang, *Langmuir*, 2009, **25**, 11032.
109 X. L. Jiang, X. F. Zhou, Y. Zhang, T. Z. Zhang, Z. R. Guo and N. Gu, *Langmuir*, 2010, **26**, 2477.
110 P. Q. Tang and J. C. Hao, *Langmuir*, 2010, **26**, 3843.
111 W. Sun, Y. C. Zhou and Z. R. Chen, *Macromol. Res.*, 2013, **21**, 414.
112 H. Sun, H. L. Li and L. X. Wu, *Polymer*, 2009, **50**, 2113.
113 W. Sun, Z. Shao and J. A. Ji, *Polymer*, 2010, **51**, 4169.
114 L. Wang, S. H. Maruf, D. Maniglio and Y. F. Ding, *Polymer*, 2012, **53**, 3749.
115 S. H. Lee, J. S. Park, B. K. Lim, C. Bin Mo, W. J. Lee, J. M. Lee, S. H. Hong and S. O. Kim, *Soft Matter*, 2009, **5**, 2343.
116 C. Deleuze, C. Derail, M. H. Delville and L. Billon, *Soft Matter*, 2012, **8**, 8559.
117 M. M. Zhang, S. T. Sun, X. D. Yu, X. H. Cao, Y. Zou and T. Yi, *Chem. Commun.*, 2010, **46**, 3553.
118 X. Y. Zhou, Z. H. Chen, Y. Z. Wang, Y. Guo, C. H. Tung, F. S. Zhang and X. W. Liu, *Chem. Commun.*, 2013, **49**, 10614.
119 J. H. Kim, M. Seo and S. Y. Kim, *Adv. Mater.*, 2009, **21**, 4130.
120 X. Xu, J. Zhang, L. Chen, X. Zhao, D. Wang and H. Yang, *Chem.-Eur. J.*, 2012, **18**, 1659.
121 R. H. Dong, J. H. Xu, Z. F. Yang, G. C. Wei, W. R. Zhao, J. L. Yan, Y. Fang and J. C. Hao, *Chem.-Eur. J.*, 2013, **19**, 13099.
122 L. P. Heng, W. Qin, S. J. Chen, R. R. Hu, J. Li, N. Zhao, S. T. Wang, B. Z. Tang and L. Jiang, *J. Mater. Chem.*, 2012, **22**, 15869.
123 E. Nomura, A. Hosoda, M. Takagaki, H. Mori, Y. Miyake, M. Shibakami and H. Taniguchi, *Langmuir*, 2010, **26**, 10266.
124 E. Ferrari, P. Fabbri and F. Pilati, *Langmuir*, 2011, **27**, 1874.
125 C. X. Cheng, Y. Tian, Y. Q. Shi, R. P. Tang and F. Xi, *Langmuir*, 2005, **21**, 6576.
126 I. O. Ucar and H. Y. Erbil, *Appl. Surf. Sci.*, 2012, **259**, 515.
127 L. A. Connal and G. G. Qiao, *Adv. Mater.*, 2006, **18**, 3024.
128 L. A. Connal and G. G. Qiao, *Soft Matter*, 2007, **3**, 837.
129 L. A. Connal, R. Vestberg, C. J. Hawker and G. G. Qiao, *Adv. Funct. Mater.*, 2008, **18**, 3315.
130 J. S. Park, S. H. Lee, T. H. Han and S. O. Kim, *Adv. Funct. Mater.*, 2007, **17**, 2315.
131 X. L. Jiang, T. Z. Zhang, L. N. Xu, C. L. Wang, X. F. Zhou and N. Gu, *Langmuir*, 2011, **27**, 5410.
132 E. Bormashenko, R. Pogreb, S. Balter and D. Aurbach, *Sci. Rep.*, 2013, **3**, 3028.
133 E. Bormashenko, S. Balter, Y. Bormashenko and D. Aurbach, *Colloid. Surf. A*, 2012, **415**, 394.
134 L. V. Govor, I. A. Bashmakov, R. Kiebooms, V. Dyakonov and J. Parisi, *Adv. Mater.*, 2001, **13**, 588.
135 T. Nishikawa, R. Ookura, J. Nishida, K. Arai, J. Hayashi, N. Kurono, T. Sawadaishi, M. Hara and M. Shimomura, *Langmuir*, 2002, **18**, 5734.
136 T. Hayakawa and S. Horiuchi, *Angew. Chem.-Int. Ed.*, 2003, **42**, 2285.
137 L. S. Wan, J. W. Li, B. B. Ke and Z. K. Xu, *J. Am. Chem. Soc.*, 2012, **134**, 95.
138 L. A. Connal, R. Vestberg, C. J. Hawker and G. G. Qiao, *Adv. Funct. Mater.*, 2008, **18**, 3706.
139 L. S. Wan, B. B. Ke, J. Zhang and Z. K. Xu, *J. Phys. Chem. B*, 2012, **116**, 40.
140 R. H. Dong, J. L. Yan, H. M. Ma, Y. Fang and J. C. Hao, *Langmuir*, 2011, **27**, 9052.
141 E. Servoli, G. A. Ruffo and C. Migliaresi, *Polymer*, 2010, **51**, 2337.
142 W. Sun, L. Y. Shen, L. M. Wang, K. Fu and J. Ji, *Langmuir*, 2010, **26**, 14236.
143 Y. Lu, Y. Ren, L. Wang, X. D. Wang and C. X. Li, *Polymer*, 2009, **50**, 2035.
144 W. J. Ge and C. H. Lu, *Soft Matter*, 2011, **7**, 2790.
145 F. Galeotti, A. Andicsova, S. Yunus and C. Botta, *Soft Matter*, 2012, **8**, 4815.
146 T. Nishikawa, M. Nonomura, K. Arai, J. Hayashi, T. Sawadaishi, Y. Nishiura, M. Hara and M. Shimomura, *Langmuir*, 2003, **19**, 6193.



 

147 S. Yamamoto, M. Tanaka, H. Sunami, E. Ito, S. Yamashita, Y. Morita and M. Shimomura, *Langmuir*, 2007, **23**, 8114.
148 H. Sun, W. Li and L. X. Wu, *Langmuir*, 2009, **25**, 10466.
149 S. R. S. Ting, E. H. Min, P. Escale, M. Save, L. Billon and M. H. Stenzel, *Macromolecules*, 2009, **42**, 9422.
150 H. Yabu, M. Takebayashi, M. Tanaka and M. Shimomura, *Langmuir*, 2005, **21**, 3235.
151 H. Yabu and M. Shimomura, *Chem. Mater.*, 2005, **17**, 5231.
152 P. C. Chen, L. S. Wan, B. B. Ke and Z. K. Xu, *Langmuir*, 2011, **27**, 12597.
153 L. S. Wan, Q. L. Li, P. C. Chen and Z. K. Xu, *Chem. Commun.*, 2012, **48**, 4417.
154 H. L. Cong, J. L. Wang, B. Yu and J. G. Tang, *Soft Matter*, 2012, **8**, 8835.
155 L. Ghannam, M. Manguian, J. Francois and L. Billon, *Soft Matter*, 2007, **3**, 1492.
156 L. Kong, R. Dong, H. Ma and J. Hao, *Langmuir*, 2013, **29**, 4235.
157 H. M. Ma, P. C. Gao, D. W. Fan, G. B. Li, D. Wu, B. Du and Q. Wei, *Phys. Chem. Chem. Phys.*, 2013, **15**, 9808.
158 J. Wang, H. X. Shen, C. F. Wang and S. Chen, *J. Mater. Chem.*, 2012, **22**, 4089.
159 H. Yabu and M. Shimomura, *Langmuir*, 2005, **21**, 1709.
160 Y. Q. Han, Q. Zhang, F. L. Han, C. X. Li, J. F. Sun and Y. Lu, *Polymer*, 2012, **53**, 2599.
161 C. Du, A. J. Zhang, H. Bai and L. Li, *ACS Macro Lett.*, 2013, **2**, 27.
162 O. Karthaus, X. Cieren, N. Maruyama and M. Shimomura, *Mater. Sci. Eng. C-Biomimetic Supramol. Syst.*, 1999, **10**, 103.
163 Y. J. Cai and B. M. Z. Newby, *Langmuir*, 2009, **25**, 7638.
164 W. F. Bu, H. L. Li, H. Sun, S. Y. Yin and L. X. Wu, *J. Am. Chem. Soc.*, 2005, **127**, 8016.
165 P. Q. Tang and J. C. Hao, *J. Colloid Interf. Sci.*, 2009, **333**, 1.
166 P. Q. Tang and J. C. Hao, *Adv. Colloid Interf. Sci.*, 2010, **161**, 163.
167 Y. Wang, Z. M. Liu, B. X. Han, H. X. Gao, J. L. Zhang and X. Kuang, *Chem. Commun.*, 2004, 800.
168 H. Cong, J. Wang, B. Yu and J. Tang, *Soft Matter*, 2012, **8**, 8835.
169 C. Greiser, S. Ebert and W. A. Goedel, *Langmuir*, 2008, **24**, 617.
170 Y. Fukuhira, H. Yabu, K. Ijiro and M. Shimomura, *Soft Matter*, 2009, **5**, 2037.
171 B. B. Ke, L. S. Wan, Y. Li, M. Y. Xu and Z. K. Xu, *Phys. Chem. Chem. Phys.*, 2011, **13**, 4881.
172 R. Daly, J. E. Sader and J. J. Boland, *Soft Matter*, 2013, **9**, 7960.
173 A. S. de Leon, A. Munoz-Bonilla, M. Fernandez-Garcia and J. Rodriguez-Hernandez, *J. Polym. Sci. Part A: Polym. Chem.*, 2012, **50**, 851.
174 (a) L. W. Zhu, L. S. Wan, J. Jin and Z. K. Xu, *J. Phys. Chem. C*, 2013, **117**, 6185; (b) L. W. Zhu, Y. Ou, L. S. Wan and Z. K. Xu, *J. Phys. Chem. B*, 2014, **118**, 845.
175 L. Li, C. K. Chen, J. Li, A. J. Zhang, X. Y. Liu, B. Xu, S. B. Gao, G. H. Jin and Z. Ma, *J. Mater. Chem.*, 2009, **19**, 2789.
176 E. Min, K. H. Wong and M. H. Stenzel, *Adv. Mater.*, 2008, **20**, 3550.
177 L. Cui, J. Peng, Y. Ding, X. Li and Y. C. Han, *Polymer*, 2005, **46**, 5334.
178 L. Cui, Y. Xuan, X. Li, Y. Ding, B. Y. Li and Y. C. Han, *Langmuir*, 2005, **21**, 11696.
179 L. S. Wan, B. B. Ke, X. K. Li, X. L. Meng, L. Y. Zhang and Z. K. Xu, *Sci. China Ser. B-Chem.*, 2009, **52**, 969.
180 A. S. de Leon, A. del Campo, M. Fernandez-Garcia, J. Rodriguez-Hernandez and A. Munoz-Bonilla, *ACS Appl. Mater. Interfaces*, 2013, **5**, 3943.
181 A. S. de Leon, A. del Campo, C. Labrugere, M. Fernandez-Garcia, A. Munoz-Bonilla and J. Rodriguez-Hernandez, *Polym. Chem.*, 2013, **4**, 4024.
182 A. Boker, Y. Lin, K. Chiapperini, R. Horowitz, M. Thompson, V. Carreon, T. Xu, C. Abetz, H. Skaff, A. D. Dinsmore, T. Emrick and T. P. Russell, *Nat. Mater.*, 2004, **3**, 302.
183 H. Li, Y. Jia, M. C. Du, J. B. Fei, J. Zhao, Y. Cui and J. B. Li, *Chem.-Eur. J.*, 2013, **19**, 5306.
184 X. F. Li, L. A. Zhang, Y. X. Wang, X. L. Yang, N. Zhao, X. L. Zhang and J. Xu, *J. Am. Chem. Soc.*, 2011, **133**, 3736.
185 Y. Q. Liu, G. B. Pan, M. Zhang and F. Li, *Mater. Lett.*, 2013, **92**, 284.
186 Z. C. Zuo, Y. J. Li, H. B. Liu and Y. L. Li, *Colloid Polym. Sci.*, 2011, **289**, 1469.
187 X. P. Xiong, W. W. Zou, Z. J. Yu, J. J. Duan, X. J. Liu, S. H. Fan and H. Zhou, *Macromolecules*, 2009, **42**, 9351.
188 P. Lan, J. Li, J. L. Gong and L. Li, *Acta Chim. Sinica*, 2012, **70**, 45.
189 V. Bahadur and S. V. Garimella, *Langmuir*, 2009, **25**, 4815.
190 C. Dorrer and J. Ruhe, *Soft Matter*, 2009, **5**, 51.
191 L. S. Wan, J. Lv, B. B. Ke and Z. K. Xu, *ACS Appl. Mater. Interfaces*, 2010, **2**, 3759.
192 X. Yang, L. W. Zhu, L. S. Wan, J. Zhang and Z. K. Xu, *J. Mater. Res.*, 2013, **28**, 642.
193 X.-M. Li, D. Reinhoudt and M. Crego-Calama, *Chem. Soc. Rev.*, 2007, **36**, 1350.
194 W. H. Ting, C. C. Chen, S. A. Dai, S. Y. Suen, I. K. Yang, Y. L. Liu, F. M. C. Chen and R. J. Jeng, *J. Mater. Chem.*, 2009, **19**, 4819.
195 N. E. Zander, J. A. Orticki, A. S. Karikari, T. E. Long and A. M. Rawlett, *Chem. Mater.*, 2007, **19**, 6145.
196 L. P. Heng, X. F. Meng, B. Wang and L. Jiang, *Langmuir*, 2013, **29**, 9491.
197 T. Nishikawa, J. Nishida, R. Ookura, S. I. Nishimura, S. Wada, T. Karino and M. Shimomura, *Mater. Sci. Eng. C-Biomimetic Supramol. Syst.*, 1999, **8-9**, 495.
198 D. Beattie, K. H. Wong, C. Williams, L. A. Poole-Warren, T. P. Davis, C. Barner-Kowollik and M. H. Stenzel, *Biomacromolecules*, 2006, **7**, 1072.
199 K. Arai, M. Tanaka, S. Yamamoto and M. Shimomura, *Colloid. Surf. A*, 2008, **313**, 530.
200 A. S. de Leon, J. Rodriguez-Hernandez and A. L. Cortajarena, *Biomaterials*, 2013, **34**, 1453.
201 T. Kawano, Y. Nakamichi, S. Fujinami, K. Nakajima, H. Yabu and M. Shimomura, *Biomacromolecules*, 2013, **14**, 1208.
202 J. B. Chaudhuri, M. G. Davidson, M. J. Ellis, M. D. Jones and X. J. Wu, *Macromol. Symp.*, 2008, **272**, 52.
203 P. M. Mendes, *Chem. Soc. Rev.*, 2008, **37**, 2512.
204 T. Chen, R. Ferris, J. Zhang, R. Ducker and S. Zauscher, *Prog. Polym. Sci.*, 2010, **35**, 94.
205 A. Nygard, T. P. Davis, C. Barner-Kowollik and M. H. Stenzel, *Aust. J. Chem.*, 2005, **58**, 595.
206 H. Yabu, Y. Hirai, M. Kojima and M. Shimomura, *Chem. Mater.*, 2009, **21**, 1787.
207 E. H. Min, S. R. S. Ting, L. Billon and M. H. Stenzel, *J. Polym. Sci. Part A: Polym. Chem.*, 2010, **48**, 3440.

208 P. Escale, L. Rubatat, C. Derail, M. Save and L. Billon, *Macromol. Rapid Commun.*, 2011, **32**, 1072.
209 P. Escale, W. Van Camp, F. Du Prez, L. Rubatat, L. Billon and M. Save, *Polym. Chem.*, 2013, **4**, 4710.



 

# Graphical Abstract

## Multiple Interfaces in Self-assembled Breath Figures

Ling-Shu Wan,* Liang-Wei Zhu, Yang Ou and Zhi-Kang Xu

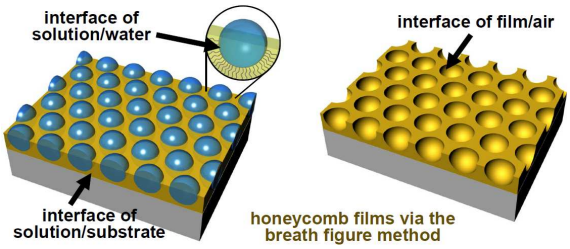


Progress in the breath figure method is reviewed by emphasizing the multiple interfaces and the applications in separation, biocatalysis, biosensing, templating, stimuli-responsive and adhesive surfaces.